

A STUDY OF THE ELECTROVISCIOUS EFFECTS  
OF COAL SUSPENSIONS IN WATER

by


Mark W. Mallett

Department of Chemical Engineering

Submitted in Partial Fulfillment of the Requirements  
of the  
University Undergraduate Fellows Program

1979-1980

Approved by:

  
Ron Darby  
Faculty Advisor

April 1980

## ABSTRACT

A Study of the Electroviscous Effects  
of Coal Suspensions in Water  
(April 1980)

Mark W. Mallett, B.S., Texas A&M University

Faculty Advisor: Dr. Ron Darby

A study was made to determine the effect of an electrolyte, namely sodium chloride (NaCl), on the apparent viscosity of coal suspensions in water. This required a fundamental study of the behavior of the second electroviscous effect on suspensions of larger particle size and more solids volume loading than has previously been done. A long term application may be in economical coal slurry pipeline development. A reduction in slurry viscosity would reduce pipeline pressure drops and power requirements.

Studies of the viscosity of coal suspensions ranging in solids volume fraction from 0.20 to 0.50 and electrolyte concentration from  $10^{-4}$  to  $10^{-1}$  molar were made using the Model R-17 Weissenberg Rheogoniometer. The variables; electrolyte concentration, solids volume fraction, and shear rate, were independently studied to determine their affect on overall suspension viscosity. In addition, tests were made to determine the charge of the ions adsorbed

on the coal particle surface, and to determine the conductivity of the electrolytic solution and suspension.

The results showed that at a low solids volume fraction, the suspension viscosity decreased with increasing electrolyte concentration to a minimum, then increased upon further electrolyte addition. The minimum occurred at an electrolyte concentration of  $10^{-3}$  molar. At a high solids volume fraction, just the opposite behavior occurred. The viscosity increased to a maximum with an electrolyte concentration of  $10^{-3}$  molar, then decreased as further electrolyte was added. Intermediate values of solids volume fraction showed no dependence on electrolyte concentration. It was also shown that the negative ion  $\text{Cl}^-$  was adsorbed by the coal particles. This indicates that further study should focus on the negatively charged ion that is added to the suspension. Some of the negative charge on the coal particles was due to the high clay content of the coal sampled. In a natural state, the clay is negatively charged. Another study of interest would look at using coal samples with varying clay content.

## ACKNOWLEDGEMENTS

I am grateful to several people for their help and encouragement during this year long research effort. Dr. Ron Darby served as my faculty advisor. He provided help and direction without "running the show" which made the project much more rewarding. John Van Zee provided help on the theory and background through his literature review on the electroviscous effects in heterogeneous fluids. Nick Stone collected the data and provided the analysis for particle size distributions. Mark O'Rosky provided help in several areas beginning with familiarization of the experimental procedure and data analysis and ending with hints on the final writing of the paper and the oral presentation. Without the contributions from each of these people, the project would not have been complete. My sincere appreciation and thanks is extended to each one of these people.

A special acknowledgement goes to Dr. Mel Friedman and the University Fellows Program for providing the opportunity to do research work as an undergraduate.

## TABLE OF CONTENTS

|                               |    |
|-------------------------------|----|
| INTRODUCTION                  | 1  |
| THEORY                        | 3  |
| APPARATUS AND PROCEDURE       | 12 |
| ANALYSIS OF RESULTS           | 19 |
| Conductivity                  | 19 |
| Charge Polarity               | 19 |
| Suspension Viscosity          | 20 |
| CONCLUSIONS                   | 61 |
| SUGGESTIONS FOR FURTHER STUDY | 62 |
| REFERENCES                    | 64 |

## LIST OF TABLES

| <u>Table</u> |   | <u>Page</u> |
|--------------|---|-------------|
| 1            | Conductivity of Electrolyte<br>Solutions and Coal Suspensions | 28          |
| 2            | Values of the Constants A and B<br>for Each Model Parameter   | 48          |

## LIST OF FIGURES

| <u>Figure</u> |   | <u>Page</u> |
|---------------|---|-------------|
| 1             | The Effect of Solid Volume Fraction on Suspension Viscosity   | 9           |
| 2             | Particle Size Distribution of a Coal-Water Suspension   | 10          |
| 3             | Effect of Shear Rate and Particle Size Distribution on Suspension Viscosity   | 11          |
| 4             | Cahn Model Electrobalance   | 16          |
| 5             | Weissenberg Rheogoniometer  | 17          |
| 6             | Concentric Cup and Bob Geometry of the Weissenberg Rheogoniometer   | 18          |
| 7             | The Effect of Shear Rate and Electrolyte Concentration on Suspension Viscosity at a Constant Solids Volume Fraction | 29          |
| 8             | The Effect of Shear Rate and Electrolyte Concentration on Suspension Viscosity at a Constant Solids Volume Fraction | 30          |
| 9             | The Effect of Shear Rate and Electrolyte Concentration on Suspension Viscosity at a Constant Solids Volume Fraction | 31          |
| 10            | The Effect of Shear Rate and Electrolyte Concentration on Suspension Viscosity at a Constant Solids Volume Fraction | 32          |
| 11            | Effect of Volume Fraction of Solids on Power Law Model for Distilled Water  | 33          |
| 12            | Effect of Volume Fraction of Solids on Bingham Model for Distilled Water  | 34          |
| 13            | Effect of Volume Fraction of Solids on Casson Model for Distilled Water   | 35          |
| 14            | Effect of Volume Fraction of Solids on Power Law Model for $10^{-1}$ Molar NaCl                                     | 36          |

| <u>Figure</u> |  | <u>Page</u> |
|---------------|--|-------------|
| 15            | Effect of Volume Fraction of Solids on Bingham Model for $10^{-1}$ Molar NaCl        | 37          |
| 16            | Effect of Volume Fraction of Solids on Casson Model for $10^{-1}$ Molar NaCl         | 38          |
| 17            | Effect of Volume Fraction of Solids on Power Law for $10^{-2}$ Molar NaCl            | 39          |
| 18            | Effect of Volume Fraction of Solids on Bingham Model for $10^{-2}$ Molar NaCl        | 40          |
| 19            | Effect of Volume Fraction of Solids on Casson Model for $10^{-2}$ Molar NaCl         | 41          |
| 20            | Effect of Volume Fraction of Solids on Power Law Model for $10^{-3}$ Molar NaCl      | 42          |
| 21            | Effect of Volume Fraction of Solids on Bingham Model for $10^{-3}$ Molar NaCl        | 43          |
| 22            | Effect of Volume Fraction of Solids on Casson Model for $10^{-3}$ Molar NaCl         | 44          |
| 23            | Effect of Volume Fraction of Solids on Power Law Model for $10^{-4}$ Molar NaCl      | 45          |
| 24            | Effect of Volume Fraction of Solids on Bingham Model for $10^{-4}$ Molar NaCl        | 46          |
| 25            | Effect of Volume Fraction of Solids on Casson Model for $10^{-4}$ Molar NaCl         | 47          |
| 26            | The Effect of Electrolyte Concentration on Parameter M From the Power Law Model      | 49          |
| 27            | The Effect of Electrolyte Concentration on Parameter N From the Power Law Model      | 50          |
| 28            | The Effect of Electrolyte Concentration on Parameter $\tau_0$ From the Bingham Model | 51          |
| 29            | The Effect of Electrolyte Concentration on Parameter $\mu_0$ From the Bingham Model  | 52          |
| 30            | The Effect of Electrolyte Concentration on Parameter $\tau_c$ From the Casson Model  | 53          |



| <u>Figure</u> |  | <u>Page</u> |
|---------------|--|-------------|
| 31            | The Effect of Electrolyte Concentration on Parameter $\mu_c$ From the Casson Model   | 54          |
| 32            | The Effect of Volume Fraction of Solids and Electrolyte Concentration on Viscosity at a Shear Rate of $1 \text{ sec}^{-1}$   | 55          |
| 33            | The Effect of Volume Fraction of Solids and Electrolyte Concentration on Viscosity at a Shear Rate of $10 \text{ sec}^{-1}$  | 56          |
| 34            | The Effect of Volume Fraction of Solids and Electrolyte Concentration on Viscosity at a Shear Rate of $100 \text{ sec}^{-1}$ | 57          |
| 35            | The Effect of Electrolyte Concentration and Shear Rate on Viscosity at a Constant Solids Volume Fraction of 0.25             | 58          |
| 36            | The Effect of Electrolyte Concentration and Shear Rate on Viscosity at a Constant Solids Volume Fraction of 0.55             | 59          |
| 37            | The Effect of Electrolyte Concentration and Shear Rate on Viscosity at a Constant Solids Volume Fraction of 0.40             | 60          |

## INTRODUCTION

In 1957, the first coal slurry pipeline in the United States began carrying coal from the Cadiz, Ohio mine to the Cleveland Electric Company. A reduction in local railroad rates eventually made coal transportation by boxcar cheaper than by pipeline. The pipeline soon closed due to financial difficulties, but the foundations for future coal pipelining had been set. Presently, one coal pipeline is in operation with six or eight others planned or proposed. Extensive research with several innovative ideas in slurry transport has been introduced in the last three years.

A major concern in pipelining is obtaining the large volume of liquid necessary to transport large amounts of coal. This is especially true where interstate pipelining is being studied. A state in the Midwest such as Montana, which has abundant coal reserves but limited water resources, cannot afford to deplete their water supply by using it to carry coal to southern states. A possible remedy is recycling the water in a parallel pipeline, but as of now this is economically infeasible. Other problems to consider are how to efficiently separate the water from the coal and what to do with the water once it has been separated.

---

The journal used as a model for this thesis was  
Chemical Engineering Science, June, 1978.

In 1977, Mr. L. J. Keller(1) patented a procedure using methanol rather than water as the transport medium. He claimed that these coal suspensions, called by the trademark name Methacoal, have properties superior to water suspensions in economical pipeline development. A study at Utah State is looking at the feasibility of using otherwise useless brine water from underground wells as the transport fluid. What might be the effect on the flow properties of coal suspensions of the ionic nature of an electrolyte such as sodium chloride(NaCl)? A possible answer to this question is the focus of this work.

The objective is to determine the effect of the concentration of an electrolyte, namely sodium chloride, on the apparent viscosity of coal in water suspensions. The application of this study is twofold. It requires a fundamental study of the behavior of the second electroviscous effect on suspensions of larger particle size and more volume loading than has previously been done. The long term application is help in economical coal slurry pipeline development. It is helpful here to distinguish between a slurry and a suspension. A slurry is slightly unstable in that unless continually agitated, the particles will partially settle out over a period of time. A suspension can be termed "pseudo homogeneous" with no particle sedimentation evident over time.

## THEORY

Dilute suspensions of rigid particles can frequently be considered Newtonian. As the particle concentration is increased, an accompanying increase in the viscosity occurs. Viscosity of a fluid refers to its resistance to flow. The suspension then shifts from Newtonian to Non-Newtonian in behavior, meaning that the viscosity of the suspension becomes dependent on the applied shear stress. In the case of a coal slurry pipeline, a minimum viscosity is desired to reduce pressure drops and power requirements yet a high yield stress is also preferred to minimize the deposit velocity and maximize slurry stability. This shift from Newtonian to Non-Newtonian behavior is attributed to particle interaction effects, such as electroviscous effects. Specifically, the electroviscous effect refers to those viscous effects associated with the distortion of the electronic double layer surrounding the suspended particles. This double layer can be thought of as a layer of charge or a buffer zone surrounding each individual particle in the suspension. It varies according to the nature and concentration of the electrolyte in solution. The changes in this double layer can be attributed to three separate effects: primary, secondary, and tertiary.

The primary effect is caused by deformation of the

outermost double layer due to fluid flow around the particles. This flow can be caused by Dorn effects where the particles migrate under the influence of gravity or electrokinetic effects where the motion is caused by a charge potential set up in the suspension. Both of these produce a shearing or tearing effect on the outermost double layer. In high solids concentrations, the primary effect is relatively small and often neglected.

The tertiary effect is attributed to shape changes in the particles' double layer due to ionization. This effect is most prominent in polymers where the ionization causes polymer chains to coil or uncoil thereby drastically changing their effective shape. In the case of rigid particles such as coal, this effect can also be neglected.

The secondary electroviscous effect is the most important and is caused by interaction between double layers on the particles. In dilute suspensions, the double layer immobilizes the liquid surrounding a particle giving it a larger effective size. This results in an effective increase in the suspension viscosity. Each particle in suspension has associated with it a particle charge or zeta potential. At high solids concentrations, these zeta potentials tend to repel particles making the suspension very unstable. The double layer acts as a buffer between these particles. A critical condition in this case then becomes the ratio of large particles to fine particles in

the suspension. The smaller particles have a double layer much greater than their actual solid diameter and essentially become isolated from any interaction with adjacent particles. This causes a reduction in the interparticle interaction and consequently in the suspension viscosity.

Research up to now has dealt with the effect of electrolytes on latexes. A good example of the texture and relative fluidity of a latex is common paint. By increasing the electrolyte content of a gelled latex, Fryling(2) reduced the viscosity from as much as several hundred thousand centipoise to less than ten. Fryling's method involved adding potassium nitrate( $KNO_3$ ) dropwise, determining the viscosity, then plotting viscosity as a function of electrolyte content. He theorized that the water molecules formed a semi-rigid envelope around the particles when adsorbed on the surface. This increase in particle size and rigidity accounted for the increased viscosity. With addition of electrolyte, the particles became fluidized thereby reducing the viscosity.

In a similar study, Brodnyan and Kelley(3) were able to obtain Newtonian flow of latexes at solids concentrations of forty percent by volume by addition of sufficient electrolyte. They indicated that Non-Newtonian behavior in suspensions of spherical particles may be entirely due to electroviscous effects. Brodnyan and Kelley attempted

a semi-quantitative explanation of the viscosity increase in terms of an effective particle radius which includes the thickness of the electronic double layer.

A more detailed look at some work by Irvin M. Krieger(4) is representative of the results in this field. Krieger added electrolytes of various valence types to deionized latices and measured their viscosities as functions of shear stress at various concentrations of polymer and electrolyte. The latexes studied ranged in solids content of from twenty to sixty percent by weight. His particle size was 0.2 microns in diameter and essentially constant. Krieger produced two major results of interest here. He determined that the viscosity diminished with increasing electrolyte concentration. In a few instances, the viscosity passed through a minimum then increased upon further electrolyte addition. Krieger also noted that the process was reversible in that adding electrolyte decreased viscosity and then removing the electrolyte from the suspension resulted in a corresponding increase in viscosity. Krieger's second result of interest was that the second electroviscous effect showed little if any specificity to electrolyte type or valence. The viscosity depended only on the total number of ions in the solution and not on the specific ion itself. He concluded that the second electroviscous effect is most dramatic when the total charge of the added cations is less than that of the colloid. Initially, the

added ions screen off part of the colloid charge causing the particles to behave as though their charge was reduced by the ion addition.

Before any correlation can be made between Krieger's results and those expected for coal suspensions, three points need to be presented. In most cases, coal suspensions have a higher solids concentration than latexes. This becomes essential in coal pipeline development since maximum solids throughput is desired. The viscosity however is greatly affected by the volume fraction of solids in the suspension. As shown in figure 1 pg 9, the ratio of the viscosity of the suspension,  $\eta$ , to that of the fluid,  $\eta_0$ , increased exponentially as the solids volume fraction increased from 0.3 to 0.4. It should also be noted that the viscosity ratios are very high indicating the much larger viscosity of the suspension than that of the liquid. The second point deals with particle size and distribution. Whereas Krieger worked with a particle size of 0.2 microns in diameter, coal suspensions have a large range of particle size and much larger diameters. Figure 2 pg. 10 shows a representative particle size distribution plot for the suspensions studied in this work. It is a plot of particle diameter in microns versus the weight percent of particles having a diameter greater than that value. The mean particle diameter was approximately fifty microns.



However, the viscosity is directly affected by the fraction of solids less than thirty microns in diameter. Figure 3 pg. 11 shows the ratio of the suspension viscosity to that of the liquid medium versus solids volume fraction less than thirty microns in diameter at four different shear rates. Each curve goes through a minimum when the fraction of solids less than thirty microns in diameter is between 0.2 and 0.4. The graph also shows the dependence of viscosity to the applied shear rate. An increase in the applied shear rate results in a large reduction in suspension viscosity. This behavior is characteristic of Non-Newtonian fluids.

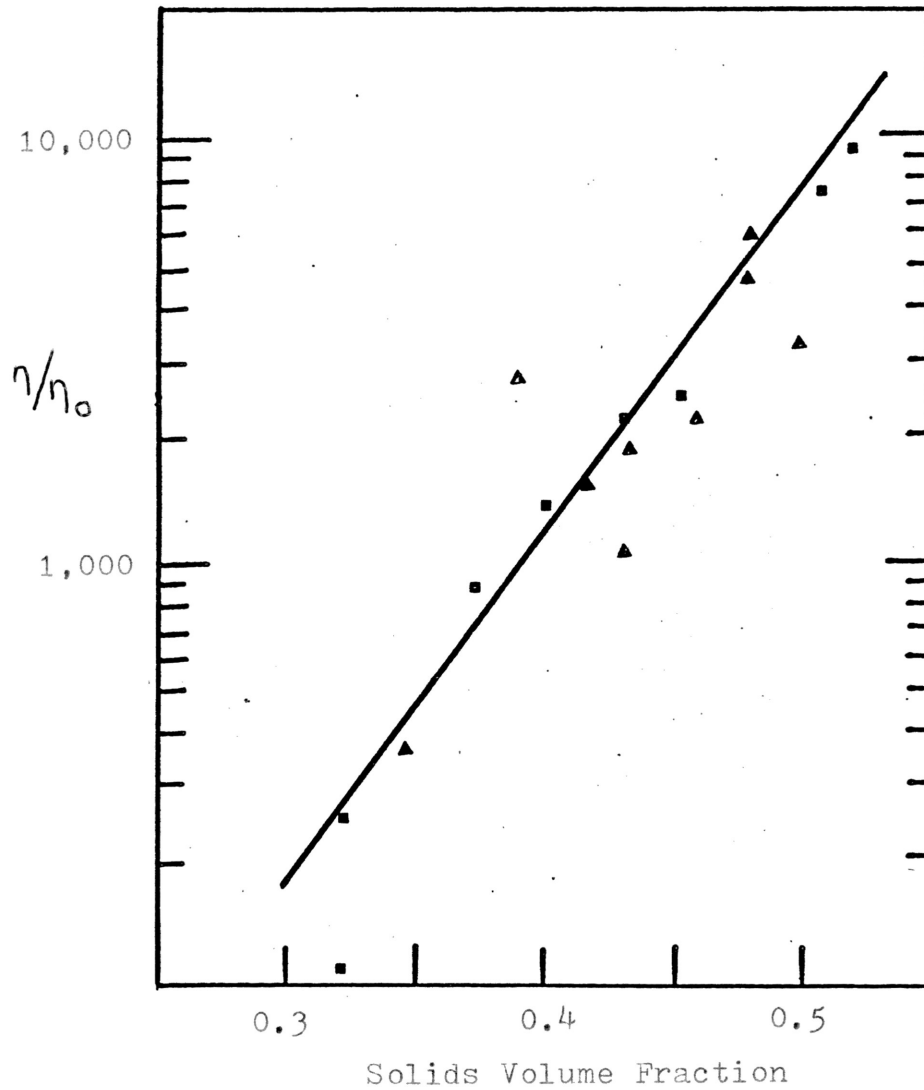


Fig. 1. The Effect of Solid Volume Fraction on Suspension Viscosity (5)

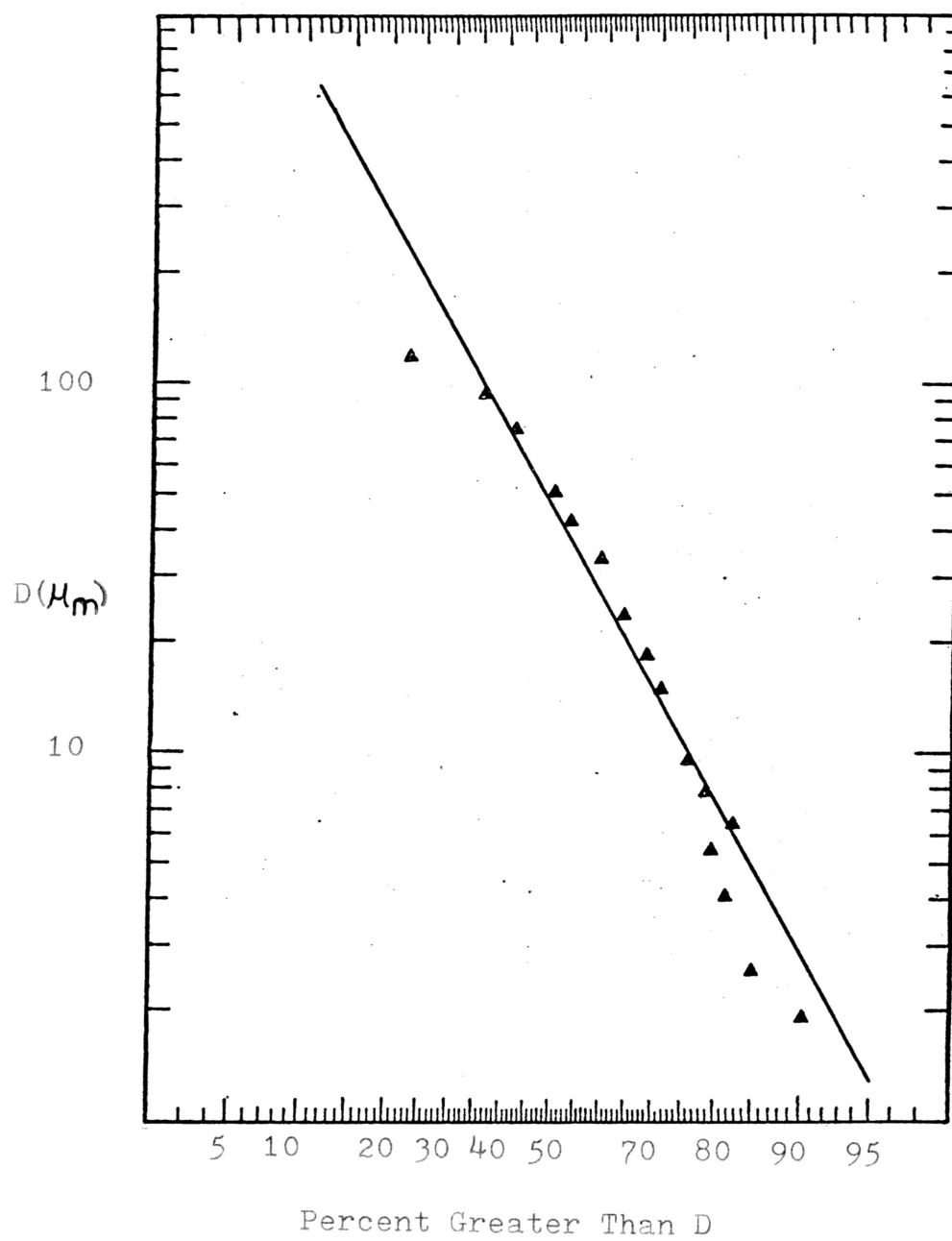


Fig. 2. Particle Size Distribution of the Coal-Water Suspension

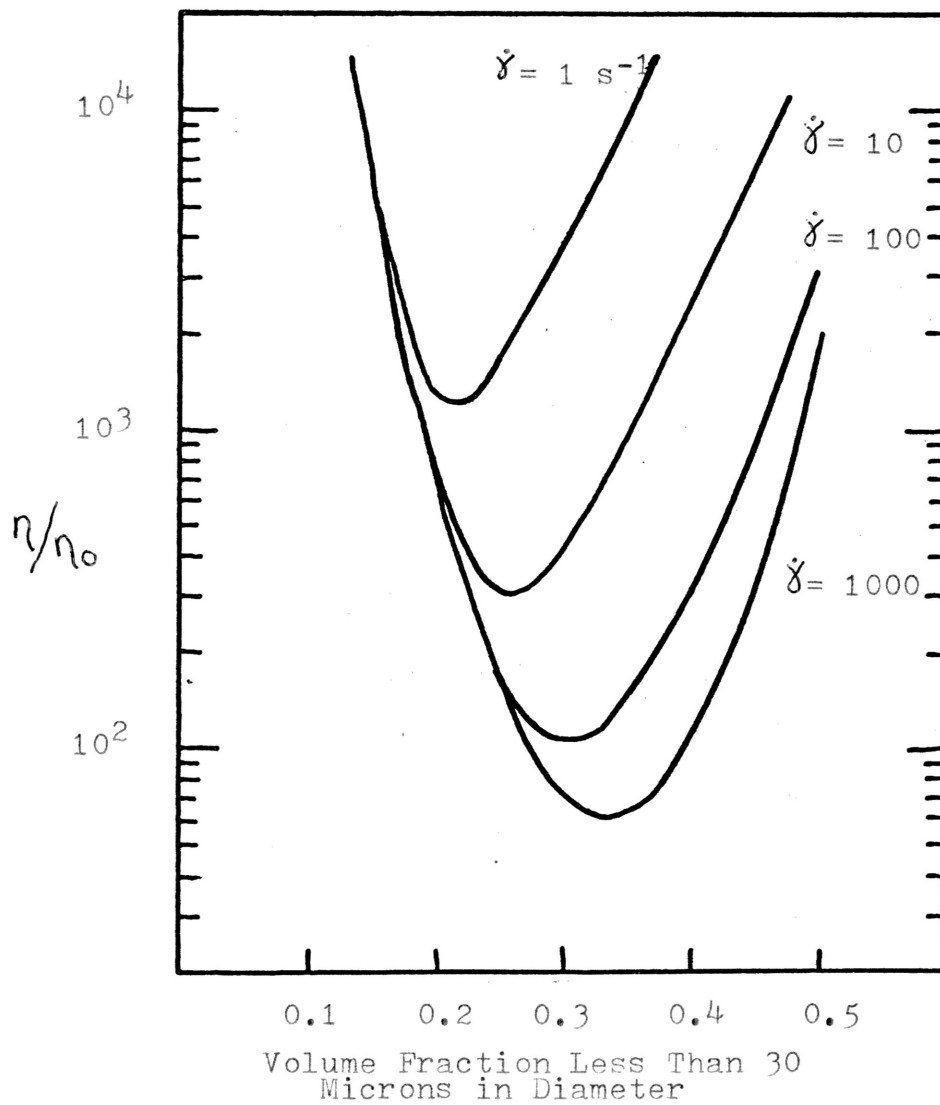


Fig. 3. Effect of Shear Rate and Particle Size Distribution on Suspension Viscosity (6)

## APPARATUS AND PROCEDURE

The lignite tested was obtained from the Big Brown Mine near Fairfield, Texas. The coal was then run through a grinder to reduce the average particle diameter to one-eighth of an inch. It was then dried in an oven for twenty four hours to remove any moisture present. This was critical to ensure that all possible active sites on the coal particles were available for interaction with the added electrolyte. The dried coal was then added to the electrolytic solution on a fifty-fifty basis by weight and blended in a Waring blender for thirty minutes to obtain the final suspension. This actually produced a particle size slightly greater than that used in commercial coal reactors. Commercial specifications require that at least ninety percent of the particles be less than seventy five microns in diameter. The samples in this study had roughly fifty eight percent less than seventy five microns in diameter as seen in figure 2.

The particle size distribution was determined using a Cahn Model RG Electrobalance, having a sensitivity of one microgram. The apparatus, shown in figure 4 pg. 16, consists of a settling column 4.8 cm in diameter, 31 cm high and filled with water. A sedimentation pan at the base of the column is attached to the balance and measures the cumulative weight of solids settling out of a uniformly dispersed

suspension as a function of time. Approximately 0.5 grams of a solid was dispersed at the top of the column with the cumulative weight of solids reaching the bottom pan recorded as a function of time on a strip chart. The average run time was from twenty four to thirty six hours. With such a small sample required, the column can be considered dilute and the particles settle with no interaction between them. The cumulative weight fraction of particles larger than a given diameter can then be plotted versus particle diameter to determine the particle size distribution of the suspension. This produced reliable values for a diameter range of from seven to one hundred microns.

Viscosity data were obtained using a Model R-17 Weissenberg Rheogoniometer, operated as a rotational viscometer with concentric cup and bob geometry. The rheogoniometer and the cup and bob are shown in figures 5-6 pgs 17-18. It is capable of producing shear rates of from 2 to 200 reciprocal seconds by varying the cup speed from 1.8 to 114 rpm. The cup has an inside diameter of 9.000 cm. and the bob has an outside diameter of 8.386 cm. Approximately 150 ml. of the suspension to be tested was poured into the bottom of the cup. The bob was then lowered into the cup forcing some of the suspension into the gap. As the cup rotated, the torque developed by shear stresses on the suspension produced a deflection on a

torsion bar and was recorded on a strip chart. The shear stress can be determined from the following equations.

$$\tau = \frac{T}{2\pi LR_i^2} \quad (1)$$

where

$$\begin{aligned} T &= \text{the torque produced} \\ L &= 5.02 \text{ cm} \\ R_i &= \text{inner bob radius} \quad 4.193 \text{ cm} \end{aligned}$$

The shear rate is given by

$$\dot{\gamma} = \frac{2\Omega\alpha^2}{\alpha^2 - 1} \quad (2)$$

where

$$\begin{aligned} \alpha &= R_o/R_i \\ R_o &= \text{outer cup radius} \quad 4.500 \text{ cm} \\ \Omega &= \text{angular velocity of cup} \end{aligned}$$

Once this shear rate is determined, it can be corrected for use in determining the apparent viscosity of a Non-Newtonian suspension by the following

$$\dot{\gamma}_c = \frac{0.1318 \dot{\gamma}}{S} \left( \frac{\alpha^{2/S}}{\alpha^{2/S} - 1} \right) \quad (3)$$

where

$$\begin{aligned} \alpha &= 1.0732 = R_o/R_i \\ S &= 1 + \text{slope of a plot of } \ln\eta \text{ vs } \ln\dot{\gamma} \end{aligned}$$

The corrected viscosity then becomes

$$\eta = \frac{\tau}{\dot{\gamma}_c} \quad (4)$$

To insure reproducibility of the data, a sequence of shear rates was used. An initial low rate of  $3 \text{ sec}^{-1}$  was used, then increased in increments to a value of  $114 \text{ sec}^{-1}$ , then reduced to a minimum value of  $1.8 \text{ sec}^{-1}$ , and finally

increased to a maximum value of  $181 \text{ sec}^{-1}$ . A total of seventeen separate points were tested for each run.

The conductivity of both the suspension and the electrolyte was determined using a digital ElectroMark Analyzer. To determine which ions were adsorbed on the coal particles, two electrodes were placed in a small amount of the suspension and a direct current applied. The movement of the particles around the oppositely charged electrodes was then observed and recorded. The solid weight fraction of the suspension was then determined using a moisture balance. This weight fraction could then be mathematically converted to a volume fraction.

As previously mentioned, the electrolyte selected for study was sodium chloride ( $\text{NaCl}$ ). It was used in concentrations of from  $10^{-1}$  to  $10^{-4}$  molar. Distilled water was used as a control. The volume fraction was initially set at 0.5 and reduced to 0.3 in three successive dilutions. With five ion concentrations at four volume fractions of solids, twenty samples were analyzed.





Fig. 4. Cahn Model Electrobalance

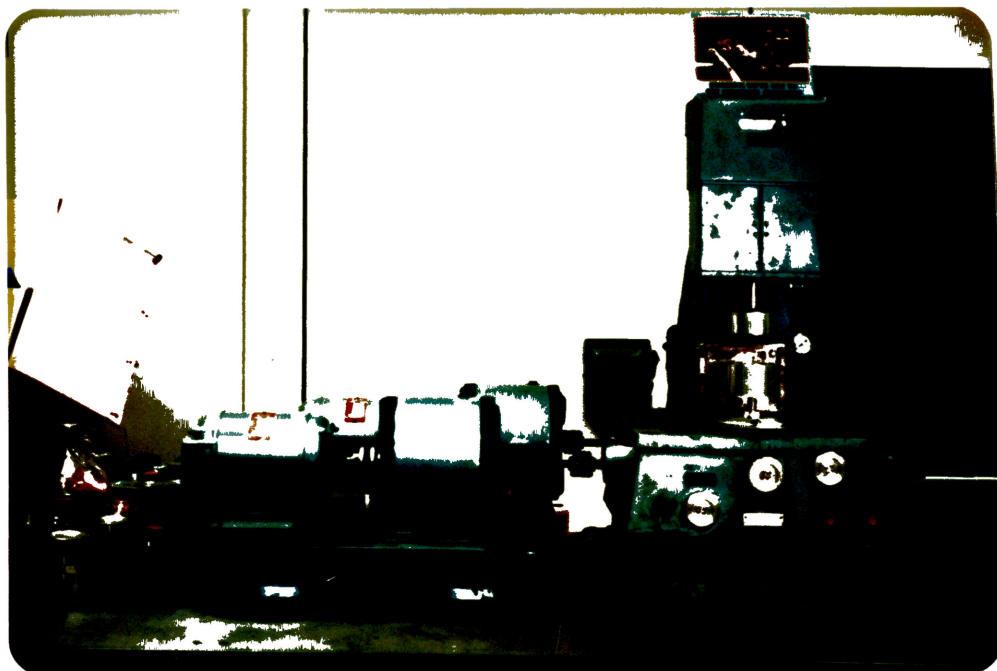


Fig. 5. Weissenberg Rheogoniometer

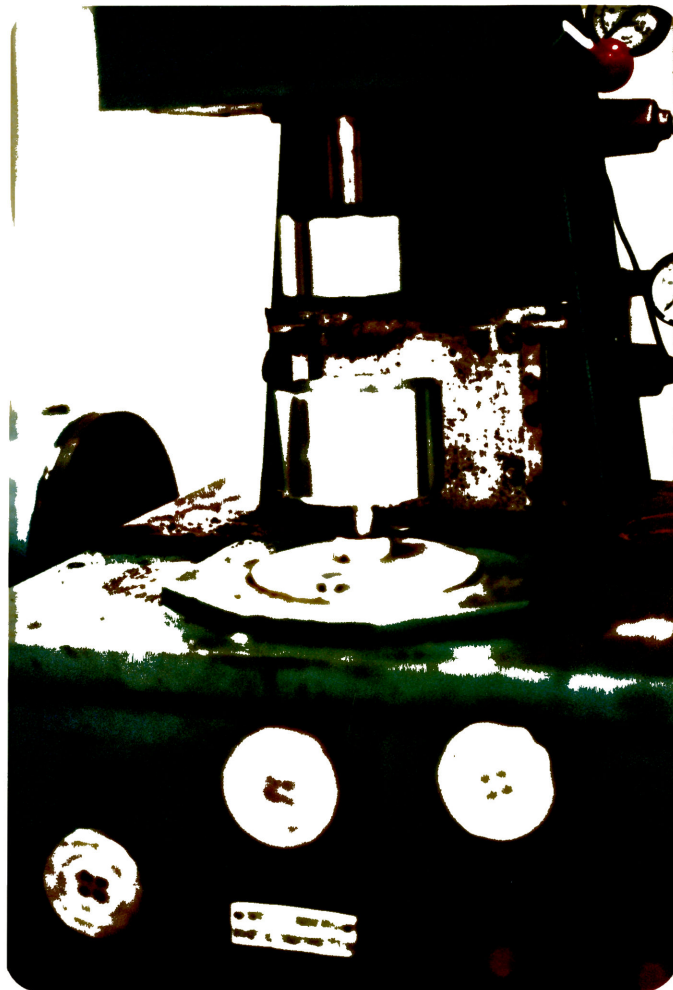


Fig. 6. Concentric Cup and Bob Geometry  
of the Weissenberg Rheogoniometer

## ANALYSIS OF RESULTS

## Conductivity

The conductivities of both the electrolyte solution and the coal suspension at each electrolyte concentration are shown in Table 1 pg. 28. The electrolyte solutions showed a decrease in conductivity of roughly one order of magnitude for each dilution. The values ranged from 13.9 micromhos for distilled water to  $10.8 \times 10^3$  micromhos for the  $10^{-1}$  molar NaCl solution. This is expected due to the increase of charged ions in the solution as the molarity is increased. The coal suspensions showed very little difference in conductivity except for the  $10^{-1}$  molar suspension which had a somewhat higher value than the other suspensions. The suspensions showed an increased conductivity over the initial electrolyte solutions in each case except for the  $10^{-1}$  molar suspension which experienced a slight reduction. Since all of the coal suspensions had conductivity values of the same order of magnitude, it can be concluded that the coal itself was so conductive that it masked any conductivity effects due to the electrolyte concentration.

## Charge Polarity

A direct current was applied to a suspension sample

containing  $10^{-1}$  molar NaCl through two bare electrodes to determine the charge on the coal particles. The particles were seen to churn vigorously and migrate away from the negative electrode. After a period of time, approximately five minutes, a cylinder or core of coal particles actually adhered or plated on the positive electrode. This indicated that the particles were negatively charged as a result of adsorbing the  $\text{Cl}^-$  ions from the NaCl. The suspension containing distilled water was sampled in the same manner and showed similar results but much less noticeable. This indicates that it is the negatively charged ions that interact with the particle double layer producing changes in the suspension viscosity.

#### Suspension Viscosity

The apparent viscosity was initially plotted versus corrected shear rate on a log-log plot for all twenty samples. These representative plots, shown in figures 7-10 pgs. 29-32, are typical of all the samples studied. Seventeen separate data points were taken for each sample and fitted by three different models.

The solid line is the Power Law Model given by

$$\tau = M \dot{\gamma}^N \quad (1)$$

To obtain viscosity values, equation (1) is divided by  $\dot{\gamma}$

leaving

$$\eta = \frac{\tau}{\dot{\gamma}} = M \dot{\gamma}^{N-1} \quad (2)$$

This model fit the data well for lower shear rates up to roughly  $100 \text{ sec}^{-1}$ . However at high shear rates ( $\dot{\gamma} \rightarrow \infty$ ), it can be seen from both equation (2) and figures 7-10 that the viscosity approaches zero.

The small dotted line is the Bingham Plastic Model given by

$$\tau = \tau_0 + \mu_0 \dot{\gamma} \quad (3)$$

Viscosity values are again obtained by dividing equation (3) by  $\dot{\gamma}$  leaving

$$\eta = \frac{\tau}{\dot{\gamma}} = \frac{\tau_0}{\dot{\gamma}} + \mu_0 \quad (4)$$

At very high shear rates, the Bingham Model predicts a limiting viscosity value of  $\mu_0$ .

The slashed line represents the Casson Model given by

$$\sqrt{\tau} = \sqrt{\tau_c} + \sqrt{\mu_c \dot{\gamma}} \quad (5)$$

Dividing equation (5) by  $\sqrt{\dot{\gamma}}$  results in

$$\sqrt{\eta} = \frac{\sqrt{\tau}}{\sqrt{\dot{\gamma}}} = \frac{\sqrt{\tau_c}}{\sqrt{\dot{\gamma}}} + \sqrt{\mu_c} \quad (6)$$

At high shear rates, the Casson Model predicts a limiting viscosity of  $\mu_c$ .

The Casson Model is generally preferred because it gives a good curve fit at both low and high shear rates. This model is also preferred because it produces upon extrapolation to high shear rates, more realistic viscosity values such as experienced in actual pipeline flow. As seen from these plots, the viscosity values

vary over as much as three decades depending upon solids volume fraction and electrolyte concentration.

Using a moisture balance, the solids weight fraction was determined directly. This is converted to a volume fraction by the following equation

$$C_V = \frac{C_W}{C_W + (1 - C_W) \rho_S / \rho_L} \quad (7)$$

where

$C_W$  = weight fraction coal  
 $C_V$  = volume fraction coal  
 $\rho_S$  = density of solid (1.45 g/cc)  
 $\rho_L$  = density of liquid (1.0 g/cc)

As discussed earlier, the viscosity is greatly affected by the solids volume fraction. Maintaining a constant solids volume fraction in order to prohibit it from masking the electrolyte concentration effects on the viscosity proved to be virtually impossible. Some method was needed to evaluate viscosity changes by varying the electrolyte concentration and holding the volume fraction constant. In order to accomplish this, each sample at a given electrolyte concentration was successively diluted to several solids fractions, over the range of 0.20 to 0.55. Each of the parameters from the three models were plotted versus solids volume fraction at each electrolyte concentration on a semi-log plot. These plots are shown in figures 11-25 pgs. 33-47. The points were then fitted to an equation of the form

$$y = Ae^{BC_V} \quad (8)$$

where

A = a constant

B = a constant

$C_V$  = the solids volume fraction

y = one of the model parameters

The values of A and B as well as the correlation factor  $r^2$  for each model parameter are shown in Table 2 pg. 48. The Bingham Model will be used for explanation. The viscosity is given by the following

$$\tau = \tau_0 + \mu_\infty \dot{\gamma} \quad (3)$$

$$\eta = \frac{\tau}{\dot{\gamma}} = \frac{\tau_0}{\dot{\gamma}} + \mu_\infty \quad (4)$$

At a constant shear rate, the viscosity  $\eta$  is a function of  $\tau_0$  and  $\mu_\infty$ . These values are representative of fluid properties. Figures 11-25 in turn give values for  $\tau_0$  and  $\mu_\infty$  as a function of the constants A, B, and  $C_V$ .

$$\tau_0 = A_1 e^{B_1 C_V} \quad (9)$$

$$\mu_\infty = A_2 e^{B_2 C_V} \quad (10)$$

These show that the model parameters have an exponential dependence on the solids volume fraction,  $C_V$ . The model parameters are also affected by the magnitude of A and B. Specifically, B shows the sensitivity of the model to changes in  $C_V$  while A indicates the relative magnitude of the respective fluid property. The greater a value of A, the larger yield stress or viscosity produced. The greater a value of B, the greater the dependence



on solids volume fraction. The values of A and B are functions of the electrolyte concentration.

As seen from the plots, the model parameters increase exponentially with increases in  $C_V$ , except for the Power Law flow index N. Within the scatter of the data, the value for N was essentially constant. This is also evident from its corresponding  $r^2$  value in Table 2. A low value of  $r^2$  indicates little dependence or a low correlation of the data to changes in  $C_V$ . Theoretically, a perfect correlation would produce an  $r^2$  value of 1.0.

The respective values of A and B for each model parameter were then plotted versus electrolyte concentration in figures 26-31 pgs. 49-54. In most cases, the values of B went through a maximum and the values of A showed a minimum. Again, the values for the Power Law flow index, N, did not correlate well as did the values for  $\mu_c$  from the Casson Model. The Bingham Model exhibited the best behavior and was used in all further analysis.

Three separate variables have been shown to affect suspension viscosity; electrolyte concentration, solids volume fraction, and shear rate. Figures 11-25 are for constant values of electrolyte concentration, and figures 26-31 are for constant values of solids volume fraction. Considering variations in all three of these would require a three dimensional plot, or a set of plots in

two dimensions.

In figures 32-34 pgs. 55-57, viscosity is plotted versus solids volume fraction for various electrolyte concentrations at shear rate values of 1, 10, 100  $\text{sec}^{-1}$ . Very little can be directly concluded from initial observation. The lines cross at a solids volume fraction range of from 0.35 to 0.45. It is apparent that no electrolyte concentration effectively reduces the suspension viscosity to a greater extent at all solids volume fractions. Further analysis does yield an indirect result that helps to verify the behavior in figures 26-31. The electrolyte concentration controls the extent which changes in solids volume fraction affect suspension viscosity. Using distilled water as the control, it can be seen that the  $10^{-3}$  molar electrolyte concentration actually enhances the effect of solids volume fraction on suspension viscosity. This is evident from the much larger slope of the  $10^{-3}$  molar line as compared to the others. The  $10^{-1}$  molar suspension, while exhibiting a slightly higher viscosity at lower solids volume fractions, reduces the viscosity at higher values of solids volume fraction while also having the smallest slope. This indicates that the  $10^{-1}$  molar electrolyte concentration reduces the sensitivity of viscosity to changes in solids volume fraction.

Figures 35-37 pgs. 58-60 plot the viscosity versus

electrolyte concentration at shear rates of 1, 10, and 100  $\text{sec}^{-1}$  at a constant solids volume fraction. The effect of the electrolyte concentration on suspension viscosity is most evident in these plots. At a low solids volume fraction of 0.25, figure 35 shows that the viscosity goes through a minimum at each shear rate at an electrolyte concentration of  $10^{-3}$  molar. At this concentration, the electrolyte isolates or buffers particle interactions thereby effectively reducing suspension viscosity. Each ion concentration reduced the viscosity as compared to the distilled sample except for the  $10^{-1}$  molar. At this high of an electrolyte concentration, the buffering effect is no longer effective and the excess ions increase particle instability.

At a high solids volume fraction of 0.55, shown in figure 36, the behavior is just opposite of that experienced at a low solids volume fraction. At each shear rate, the viscosity produces a maximum at an electrolyte concentration of  $10^{-3}$  molar. At these higher solids volume fractions, the individual particles are crowded together. This crowding effect enhances particle interaction. At a concentration of  $10^{-3}$  molar, the effect of the ion adsorption is greatest. The particle surfaces become saturated with adsorbed ions at this concentration. Below this value, as adsorbed ion concentration builds up on particles, electrostatic forces cause an effective increase in the

radius of influence of the particle. This has the same effect as increasing the solids volume fraction. At higher electrolyte concentrations, the ions in solution effectively "short out" this field.

Figure 37 shows the effect of electrolyte concentration on suspension viscosity at an intermediate solids volume fraction of 0.40. Within the scatter of the data, the viscosity shows essentially no dependence on electrolyte concentration. At this solids volume fraction, the effects present at low and high solids volume fraction cancel each other out producing viscosity values that differ very little from the distilled water values.

TABLE 1

Conductivity of Electrolyte Solutions  
and Coal Suspensions

| <u>Solution Concentration</u><br>(molarities) | <u>Conductivity</u><br>(micromhos) |
|---|------------------------------------|
| 10 <sup>-1</sup>                              | 10,800.                            |
| 10 <sup>-2</sup>                              | 1,388.                             |
| 10 <sup>-3</sup>                              | 148.9                              |
| 10 <sup>-4</sup>                              | 17.7                               |
| Distilled                                     | 1.39                               |

| <u>Suspension Concentration</u><br>(molarities) | <u>Conductivity</u><br>(micromhos) |
|---|------------------------------------|
| 10 <sup>-1</sup>                                | 6,470                              |
| 10 <sup>-2</sup>                                | 2,240                              |
| 10 <sup>-3</sup>                                | 2,080                              |
| 10 <sup>-4</sup>                                | 2,140                              |
| Distilled                                       | 1,695                              |

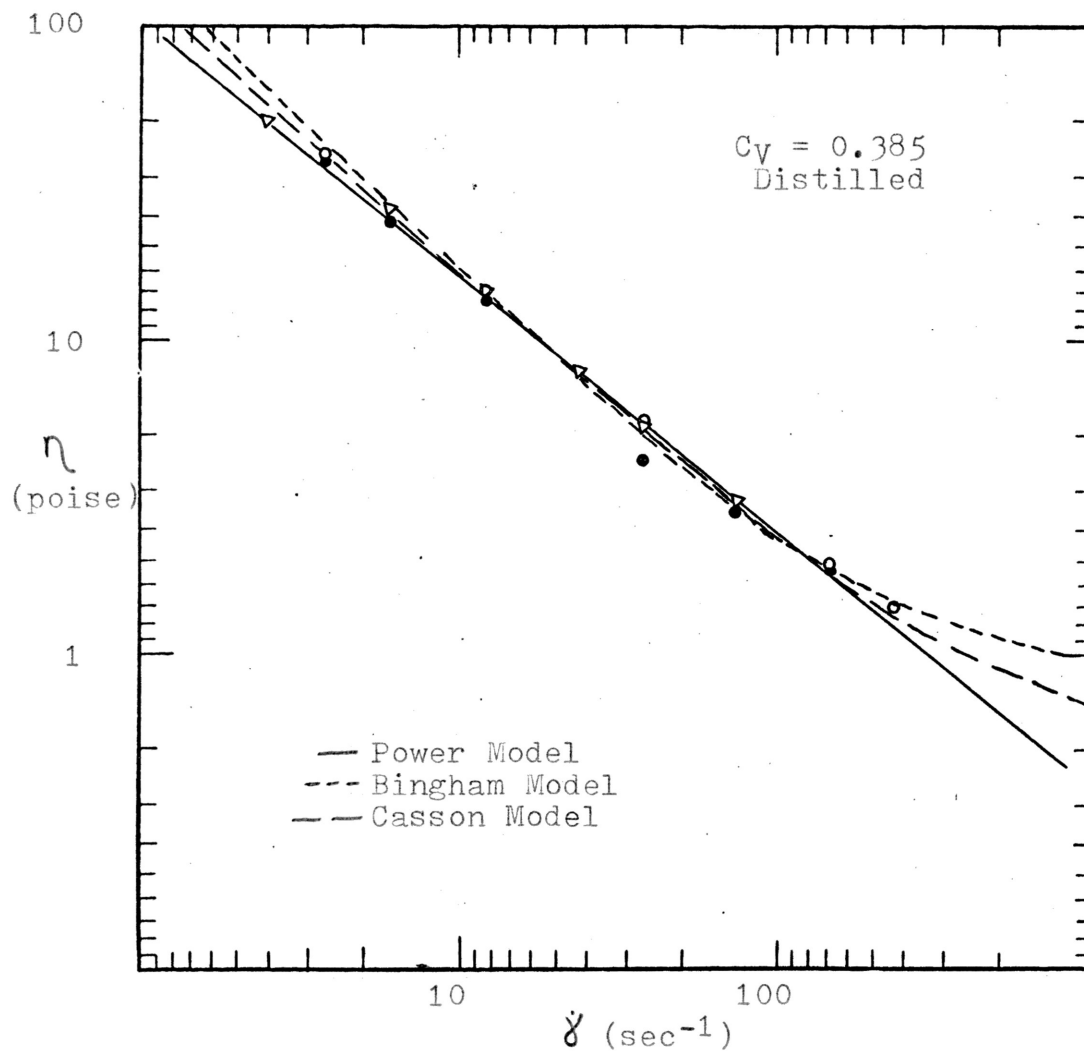


Fig. 7. The Effect of Shear Rate and Electrolyte Concentration on Suspension Viscosity at a Constant Solids Volume Fraction

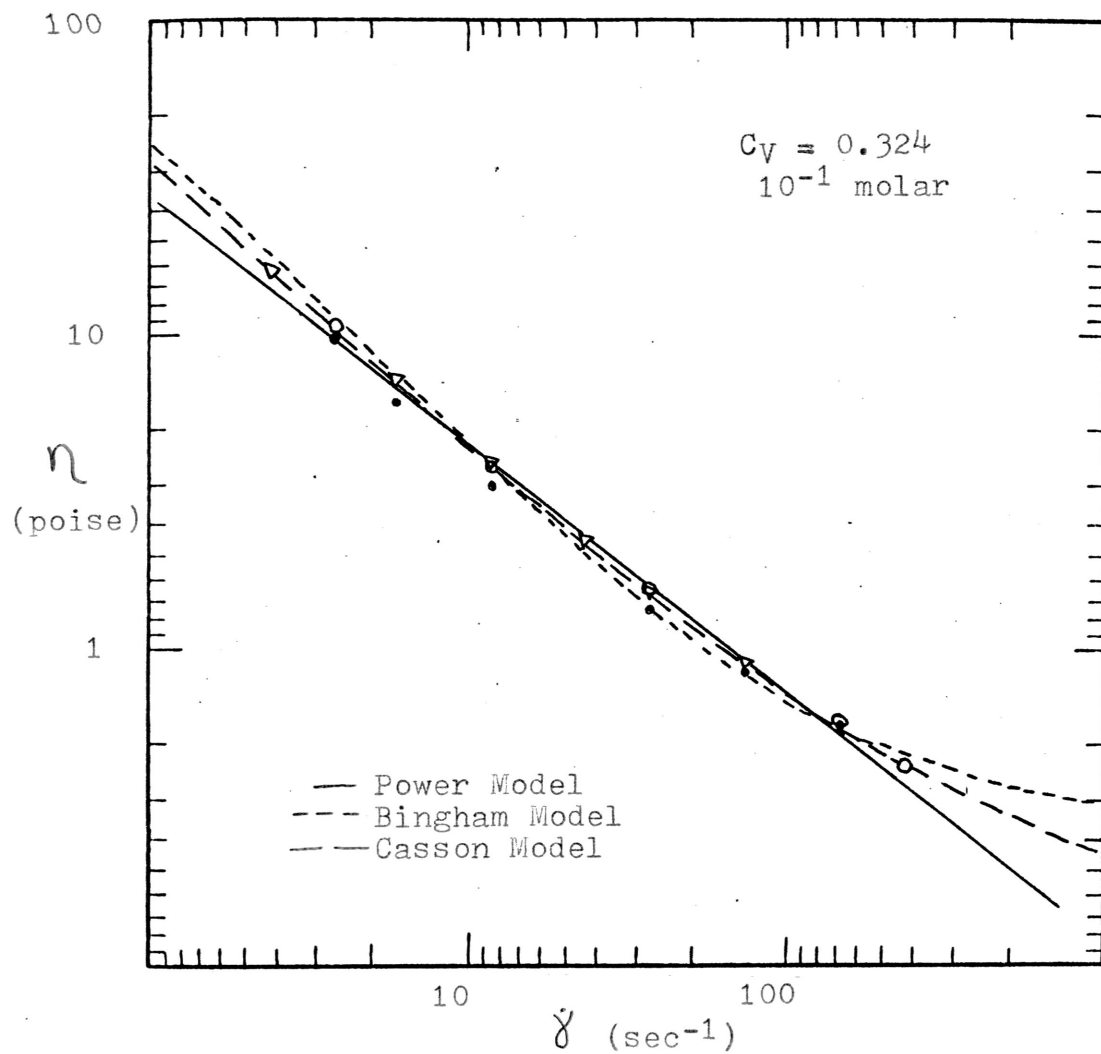


Fig. 8. The Effect of Shear Rate and Electrolyte Concentration on Suspension Viscosity at a Constant Solids Volume Fraction

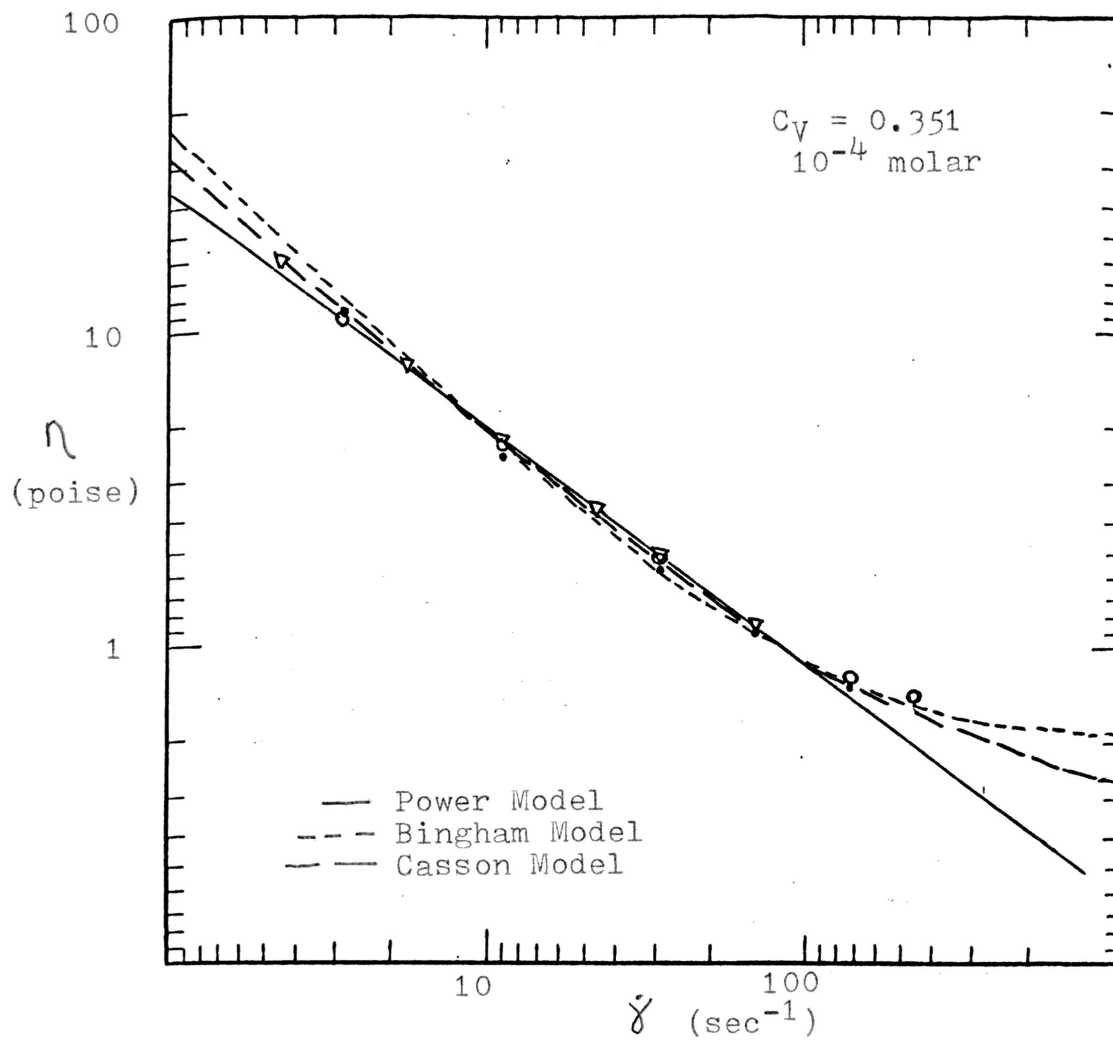


Fig. 9. The Effect of Shear Rate and Electrolyte Concentration on Suspension Viscosity at a Constant Solids Volume Fraction



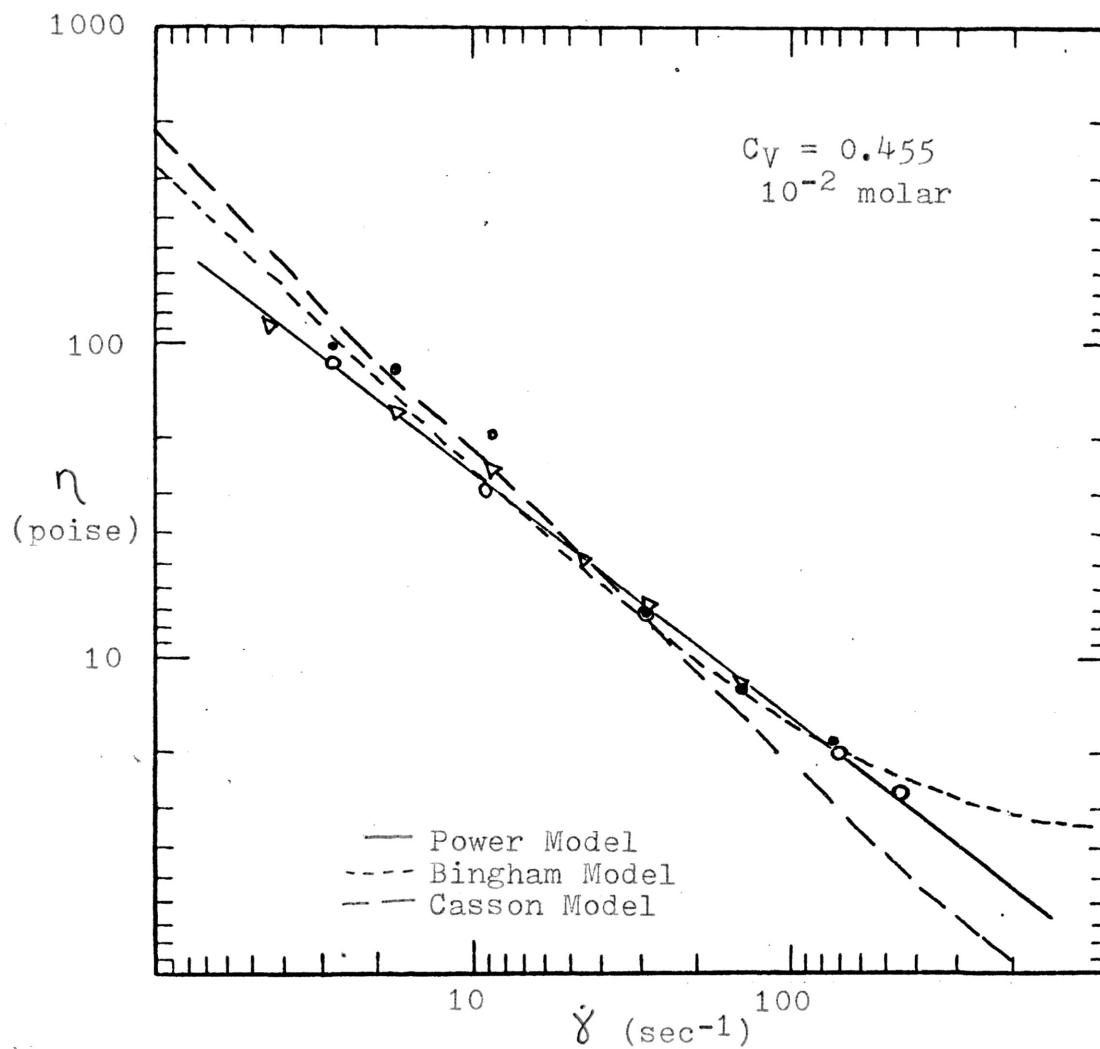


Fig. 10. The Effect of Shear Rate and Electrolyte Concentration on Suspension Viscosity at a Constant Solids Volume Fraction

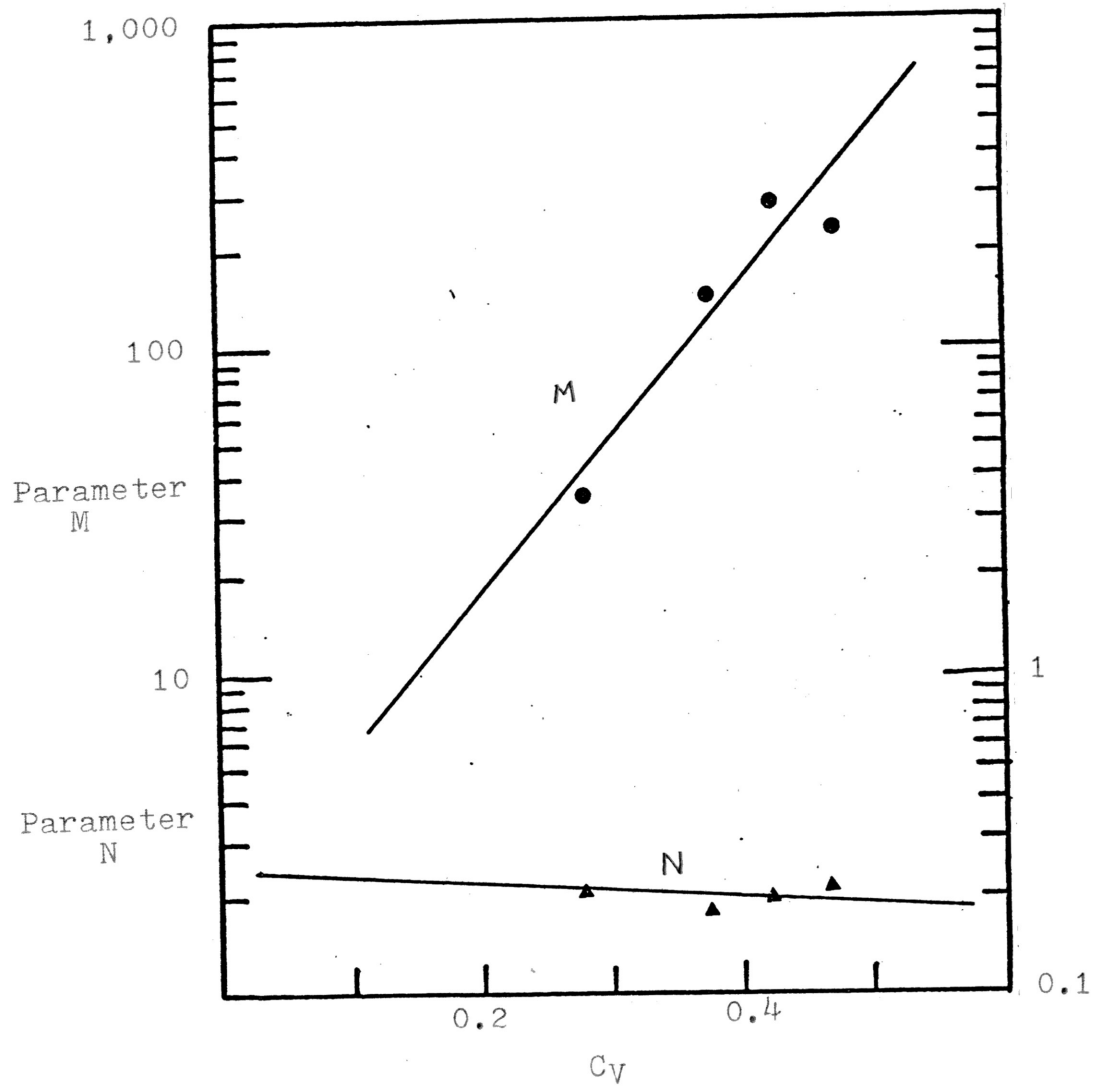


Fig. 11 Effect of Volume Fraction of Solids on Power Law Model For Distilled Water

Note: The values on the right hand side abscissa correspond to the magnitude of the lower parameter.

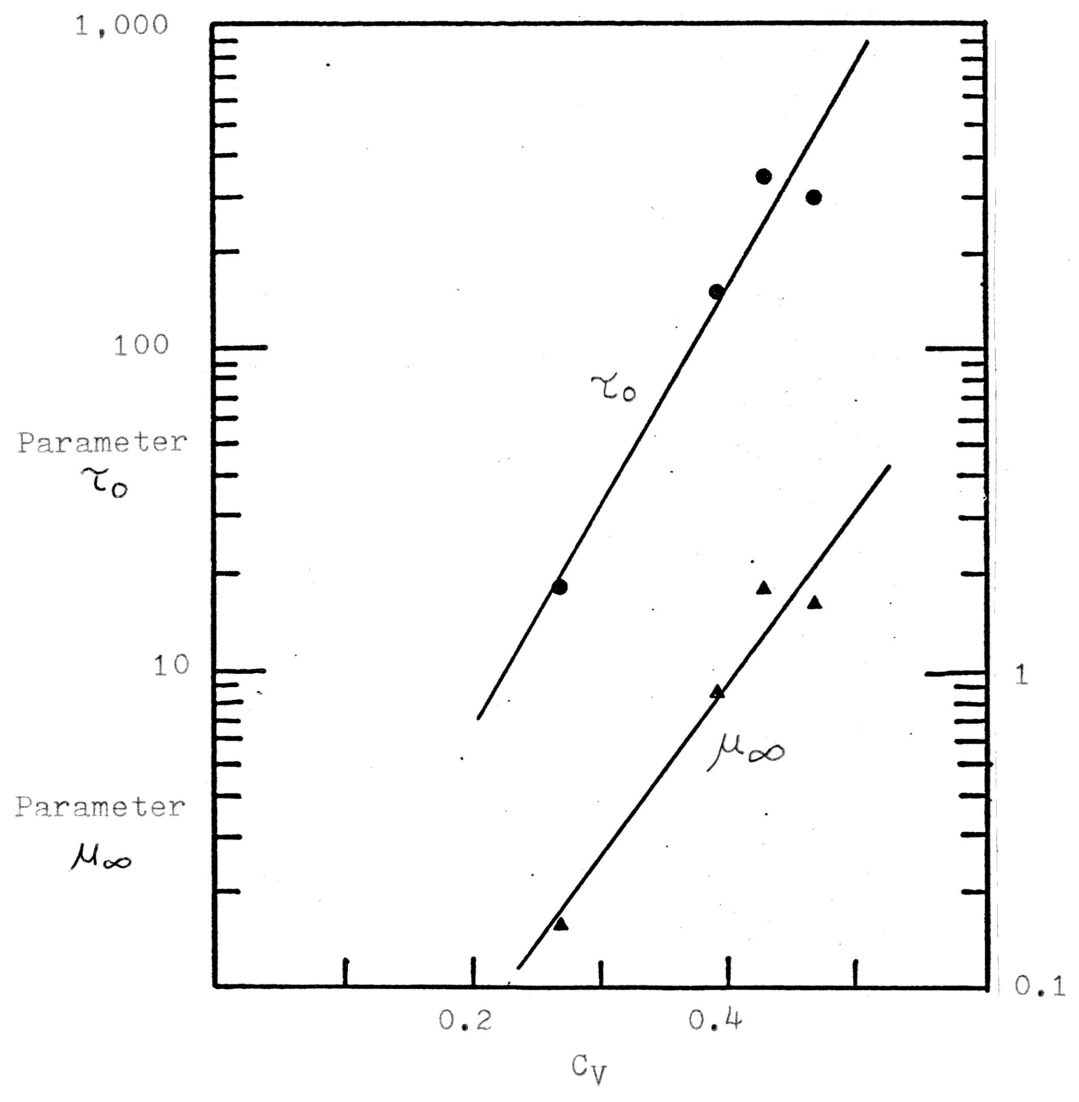


Fig. 12. Effect of Volume Fraction of Solids on Bingham Plastic Model For Distilled Water

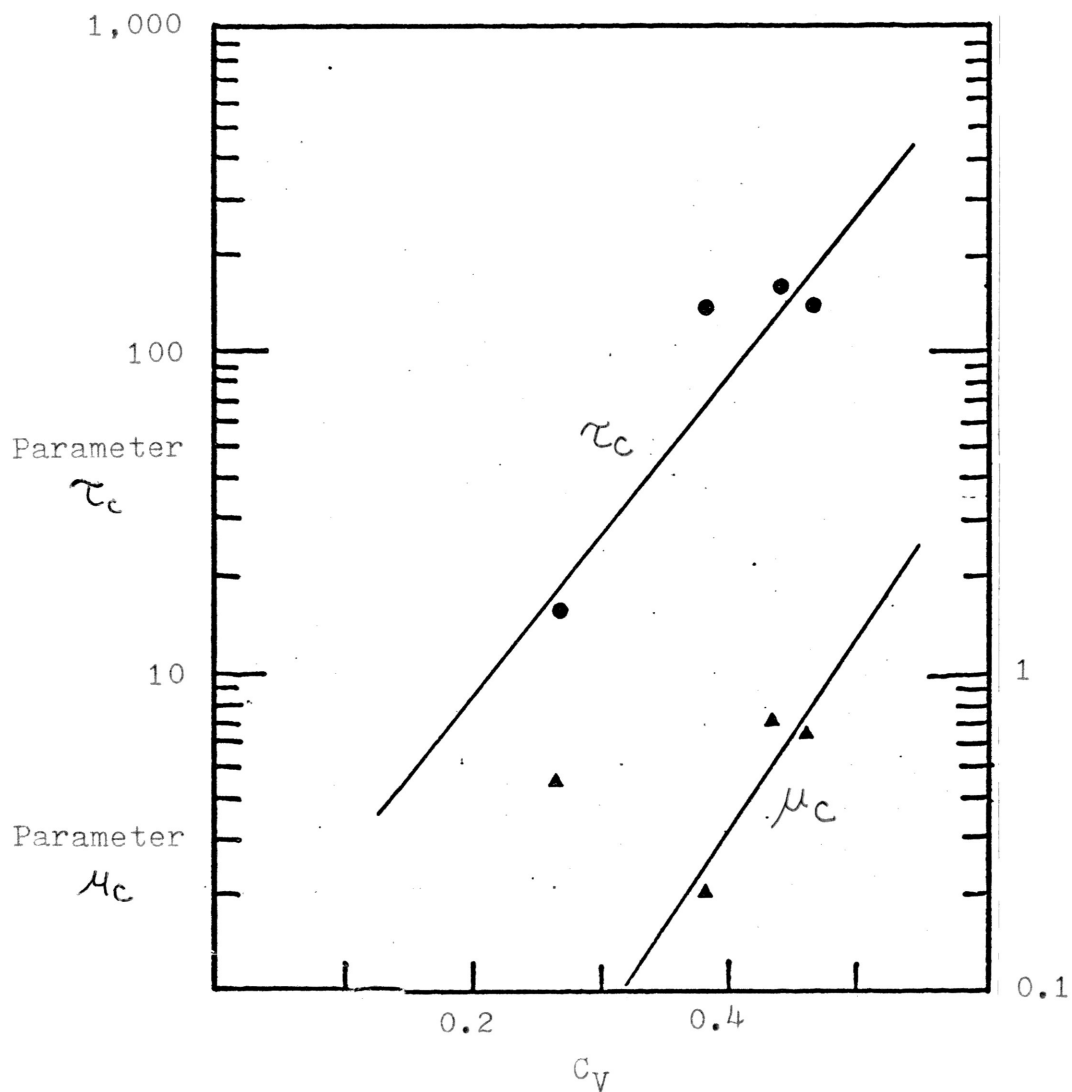


Fig. 13. Effect of Volume Fraction of Solids on Casson Model For Distilled Water

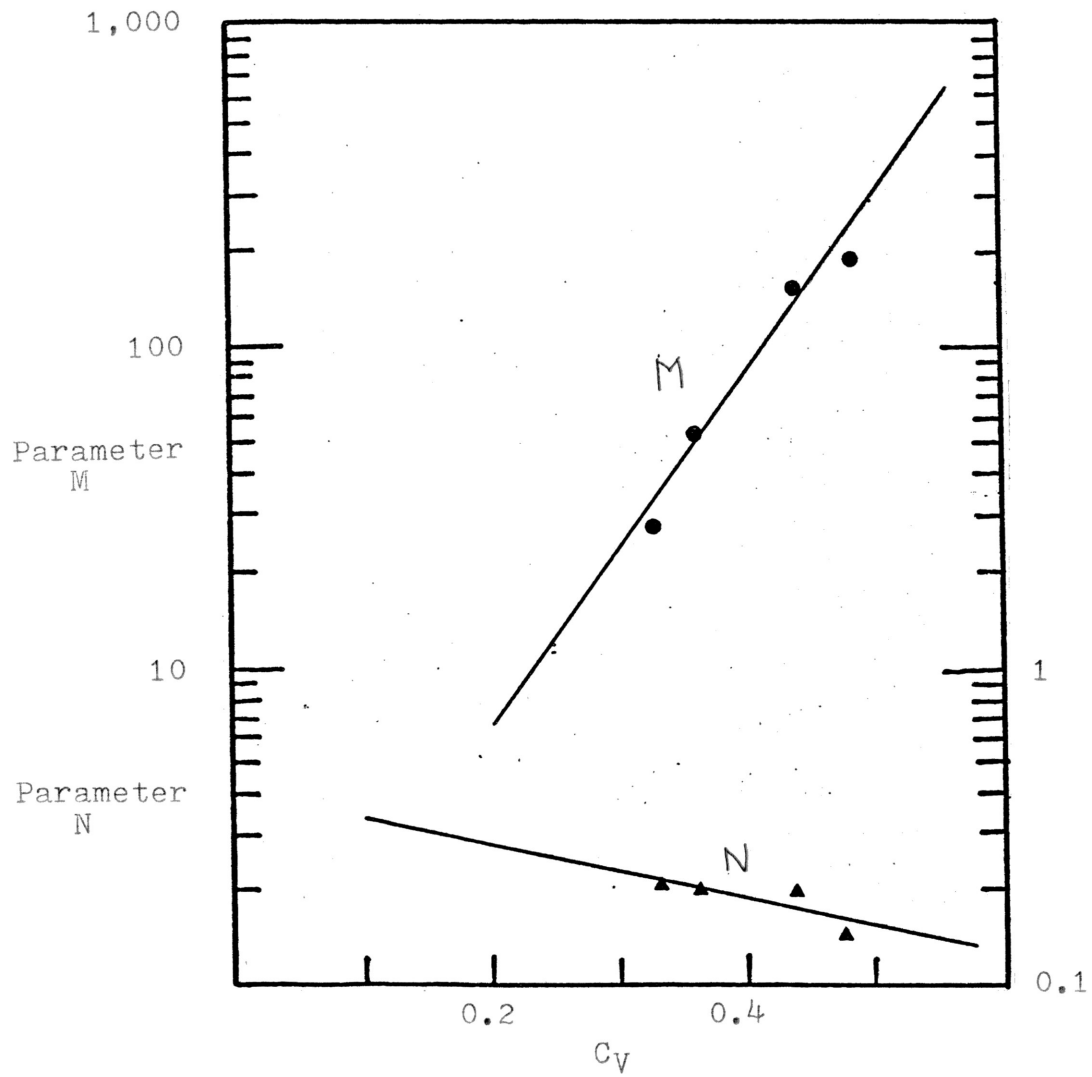


Fig. 14. Effect of Volume Fraction of Solids on Power Law Model For  $10^{-1}$  Molar NaCl

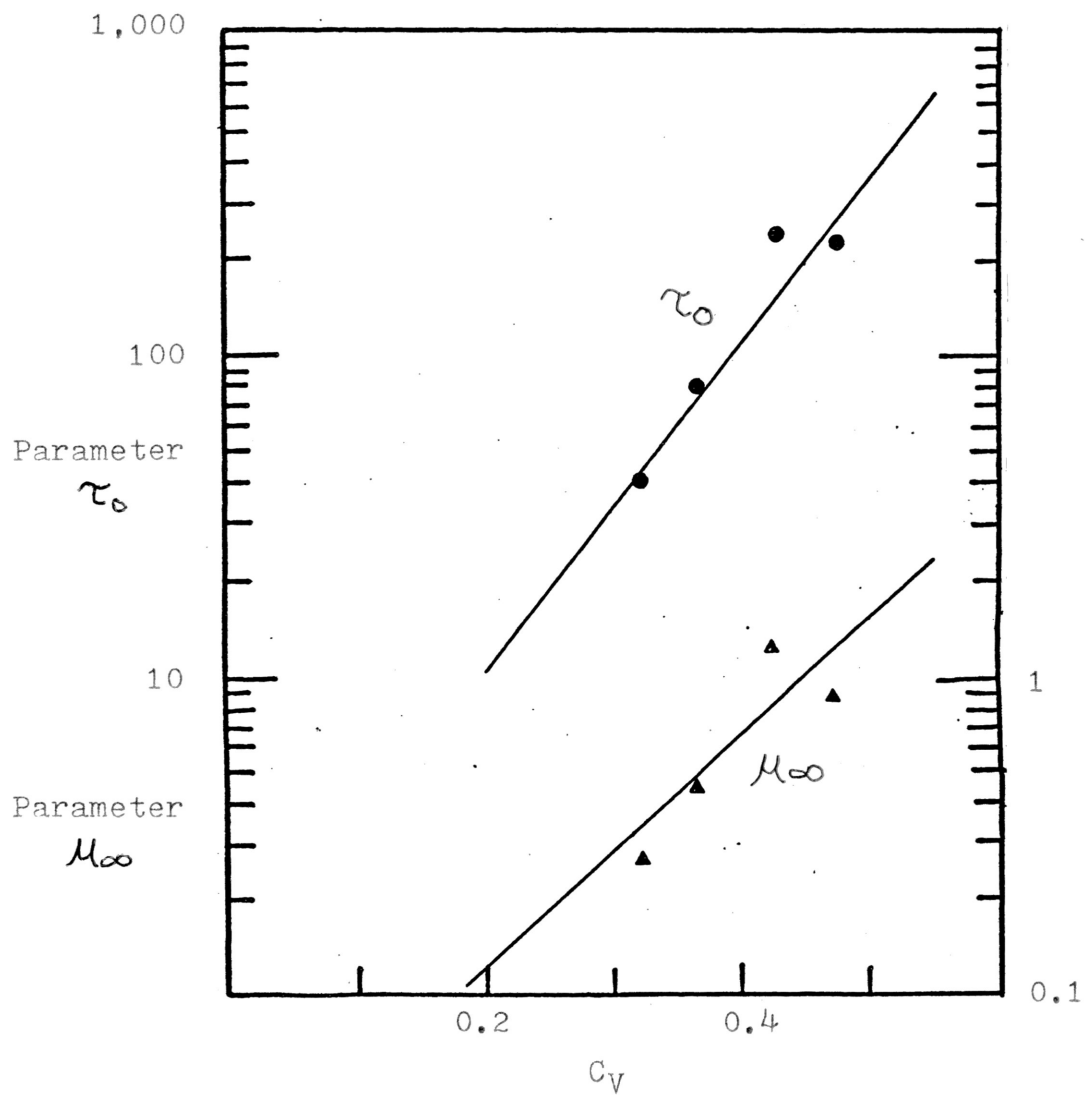


Fig. 15. Effect of Volume Fraction of Solids on Bingham Plastic Model For  $10^{-1}$  Molar NaCl

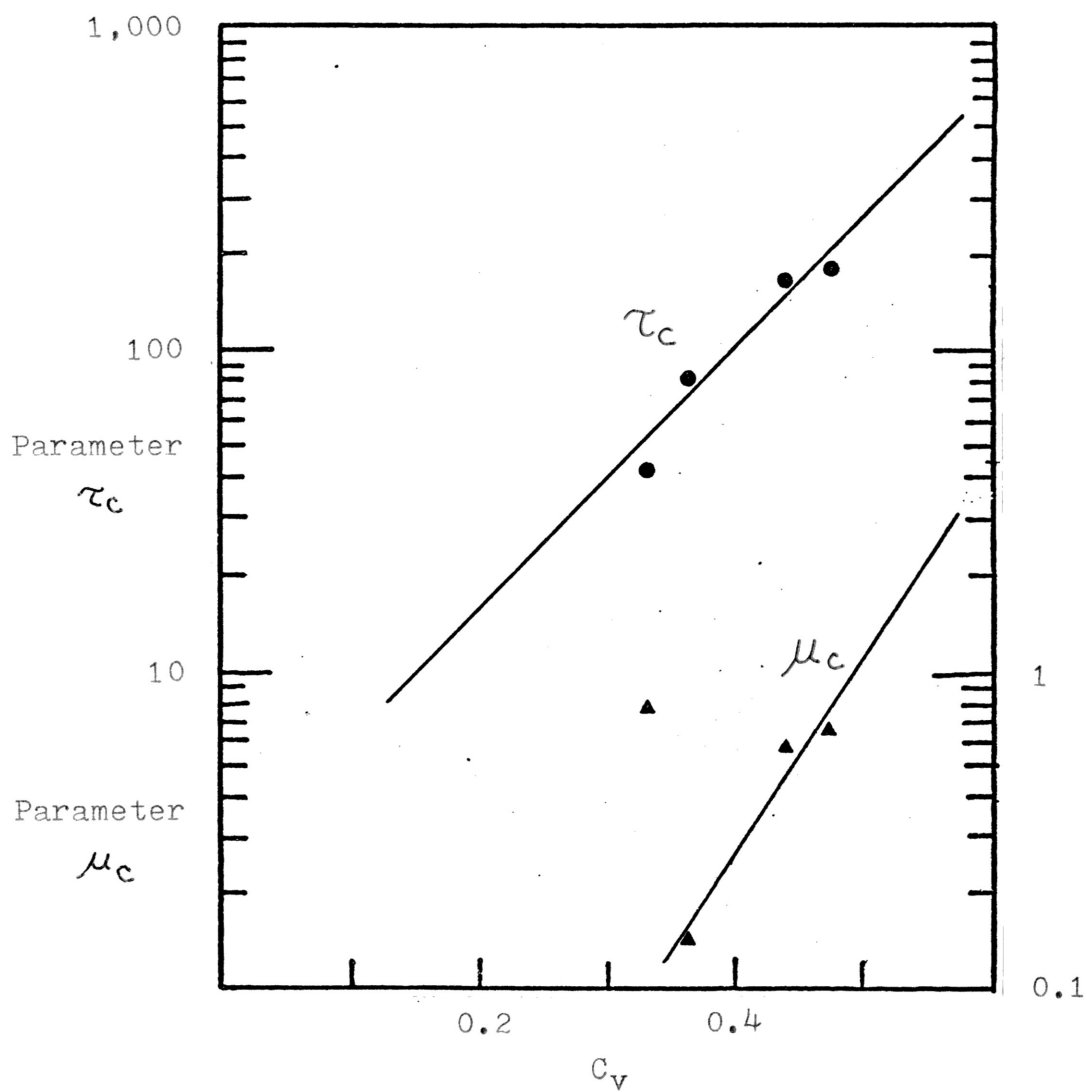


Fig. 16. Effect of Volume Fraction of Solids on Casson Model For  $10^{-1}$  Molar NaCl

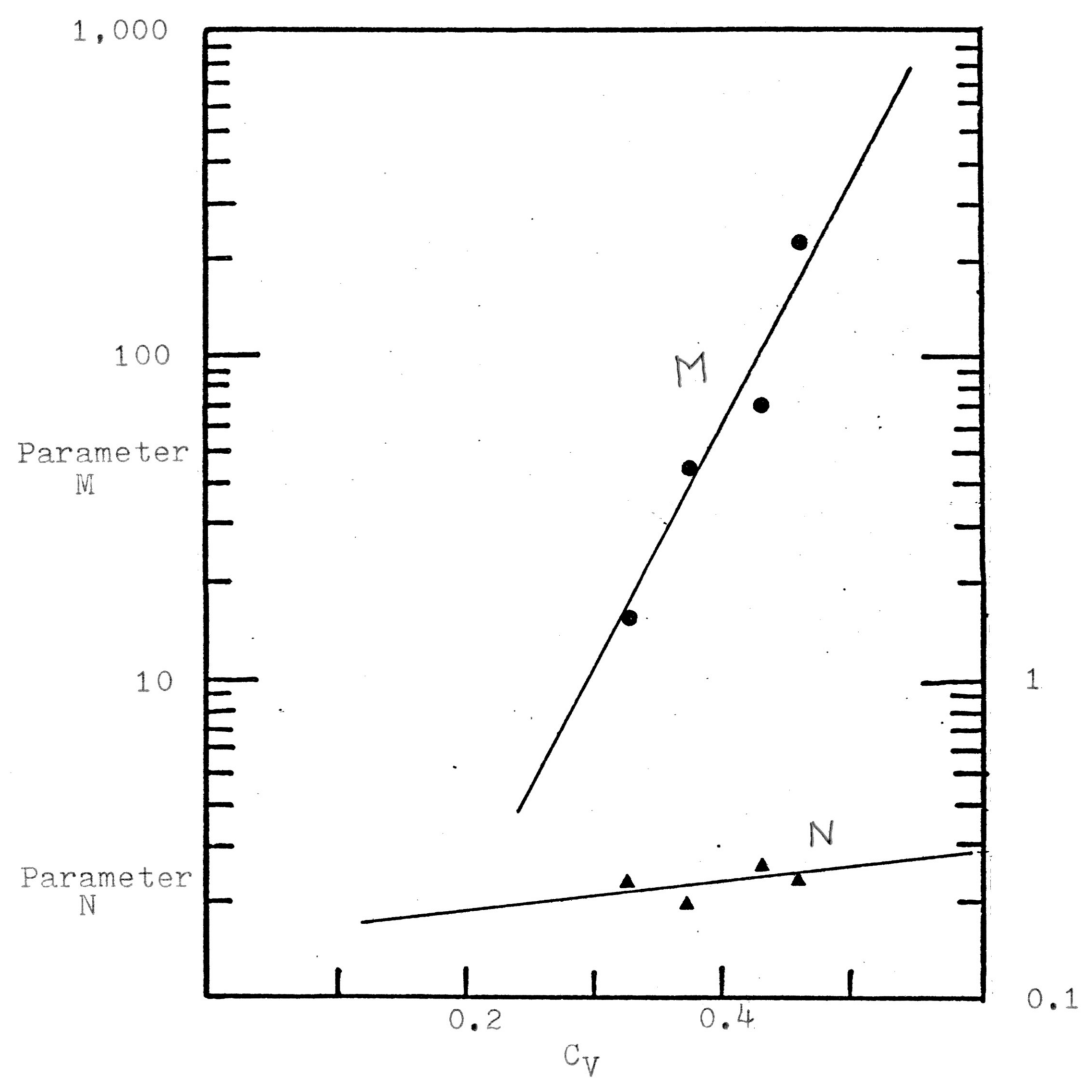


Fig. 17. Effect of Volume Fraction of Solids on Power Law Model For  $10^{-2}$  Molar NaCl



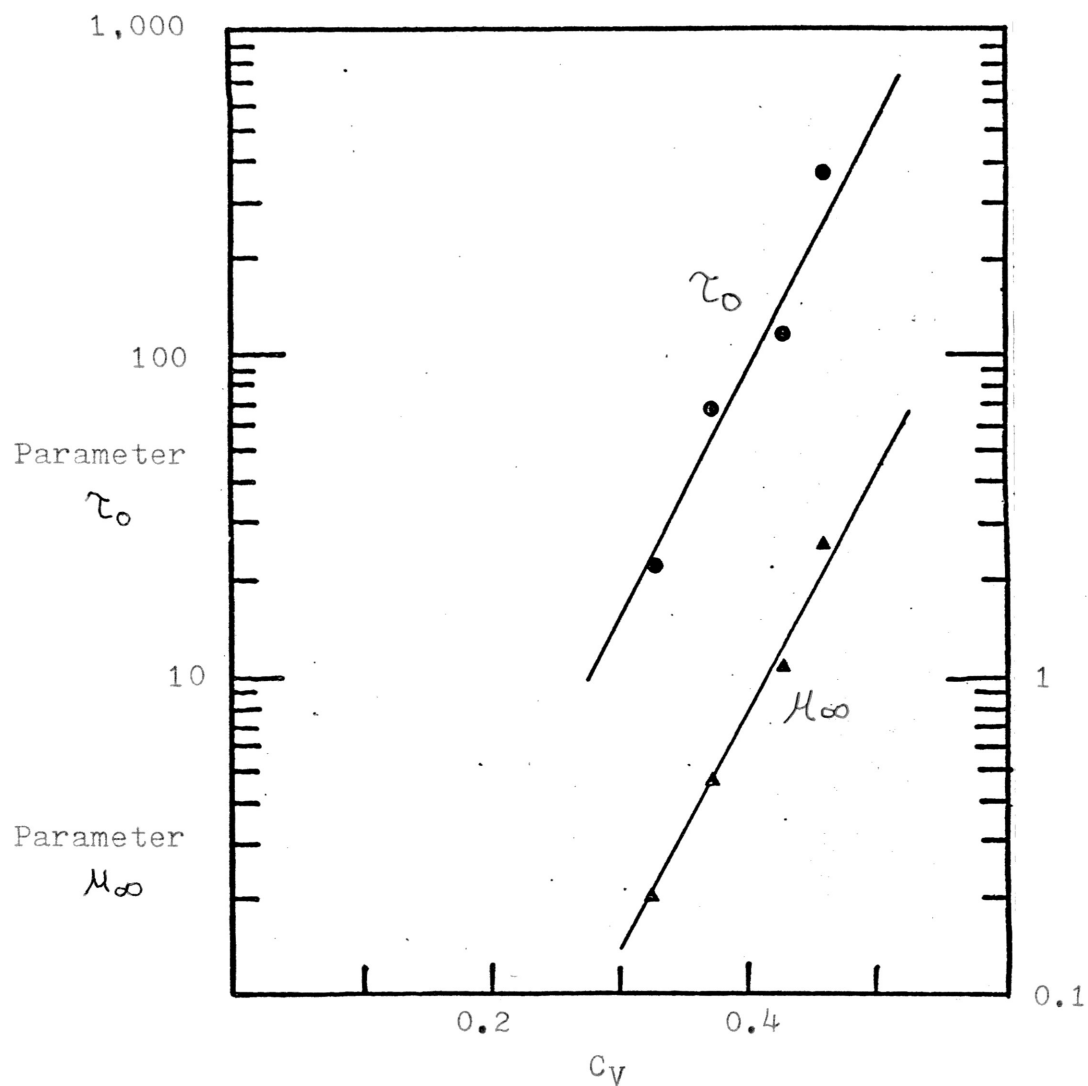


Fig. 18. Effect of Volume Fraction of Solids on Bingham Plastic Model For  $10^{-2}$  Molar NaCl

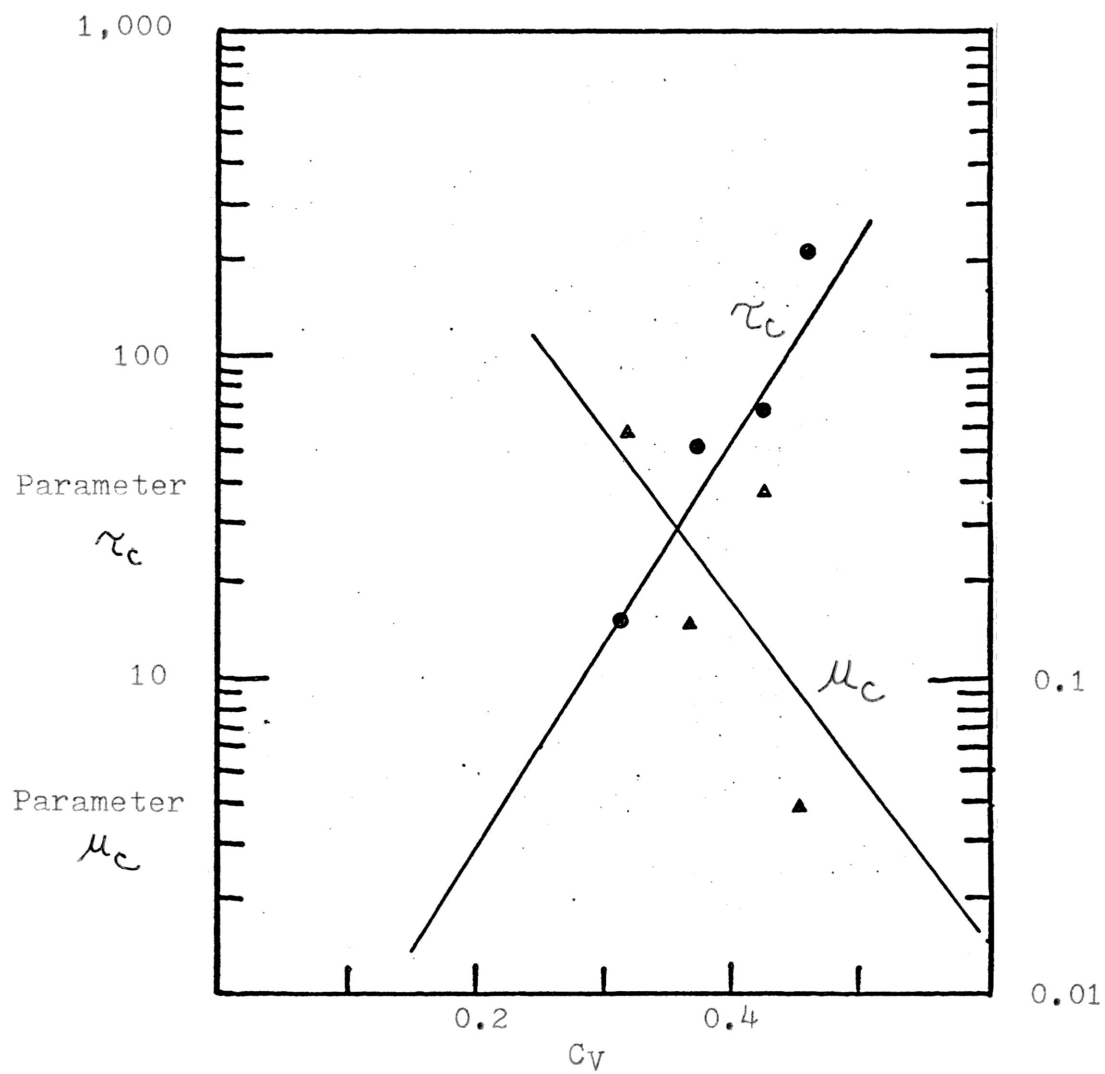


Fig. 19. Effect of Volume Fraction of Solids on Casson Model For  $10^{-2}$  Molar NaCl

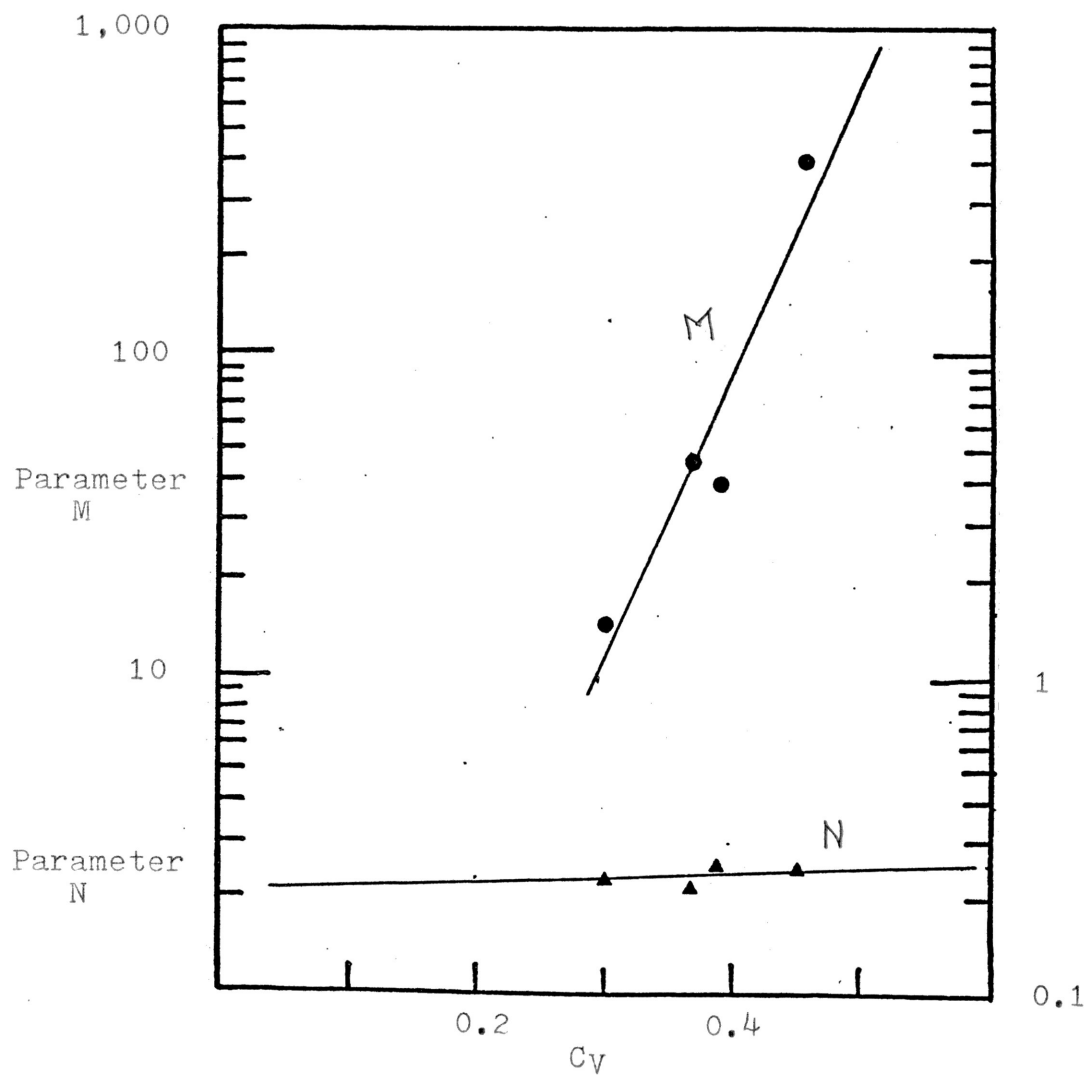


Fig. 20. Effect of Volume Fraction of Solids on Power Law Model For  $10^{-3}$  Molar NaCl

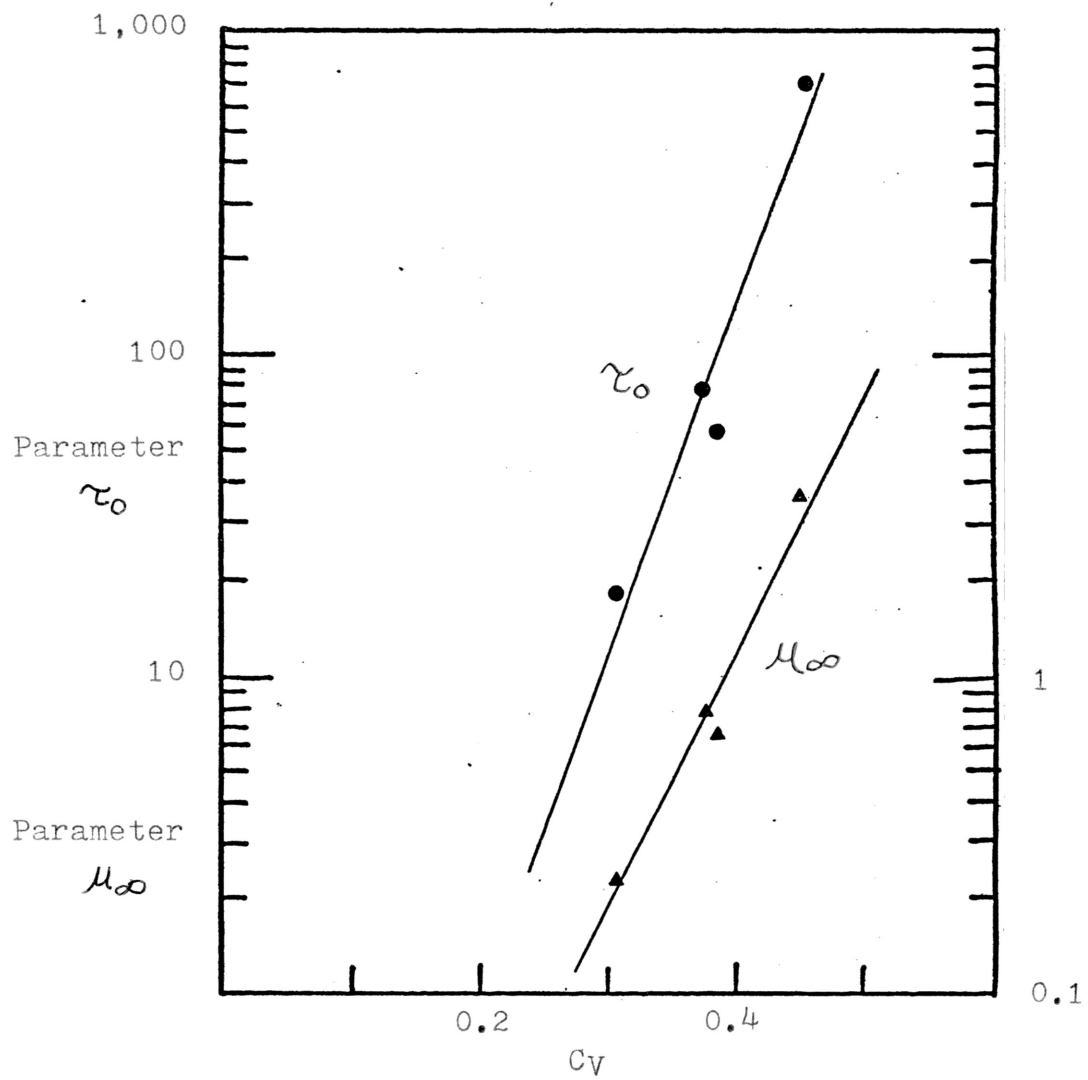


Fig. 21. Effect of Volume Fraction of Solids on Bingham Plastic Model For  $10^{-3}$  Molar NaCl

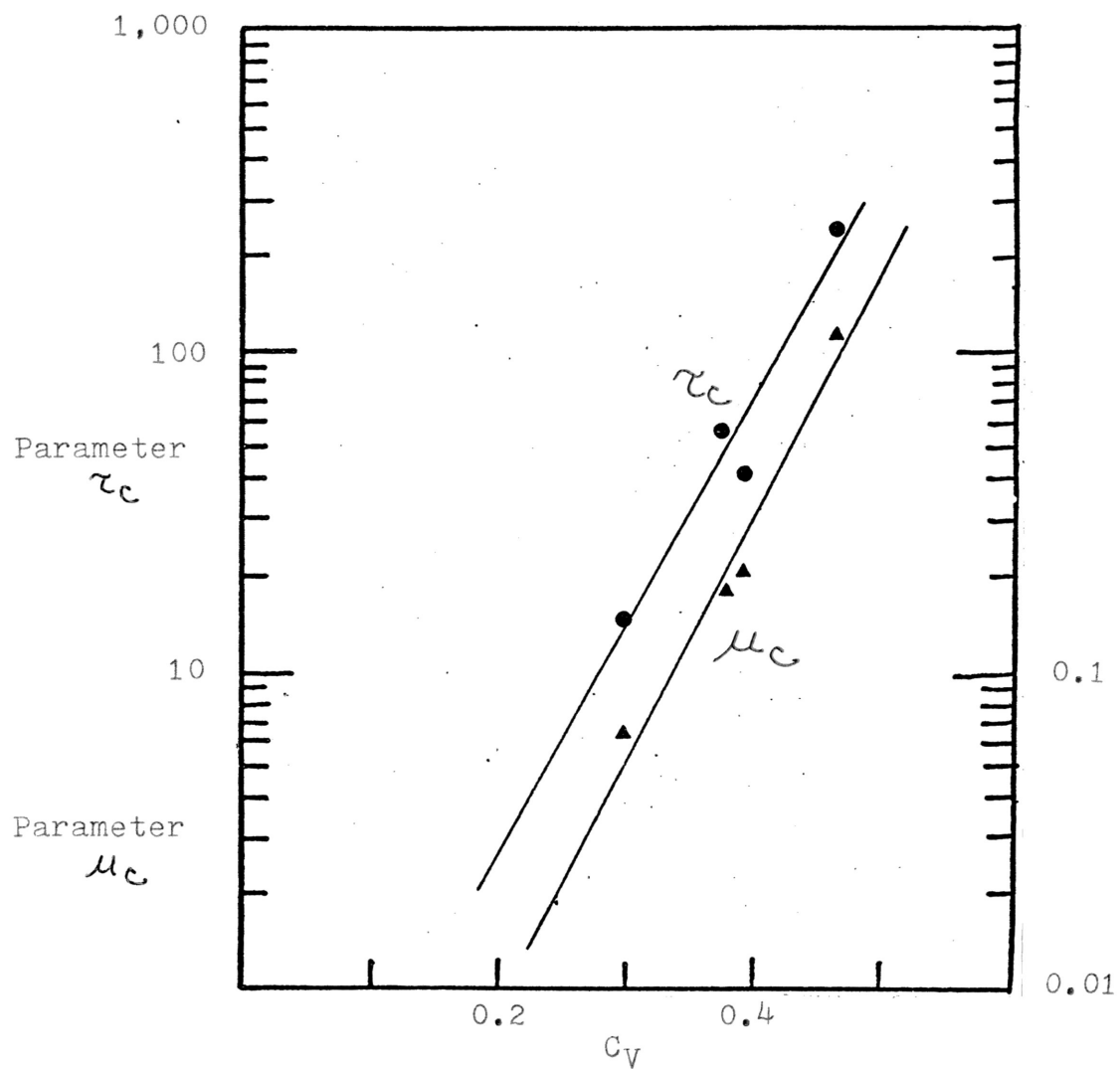


Fig. 22. Effect of Volume Fraction of Solids on Casson Model For  $10^{-3}$  Molar NaCl

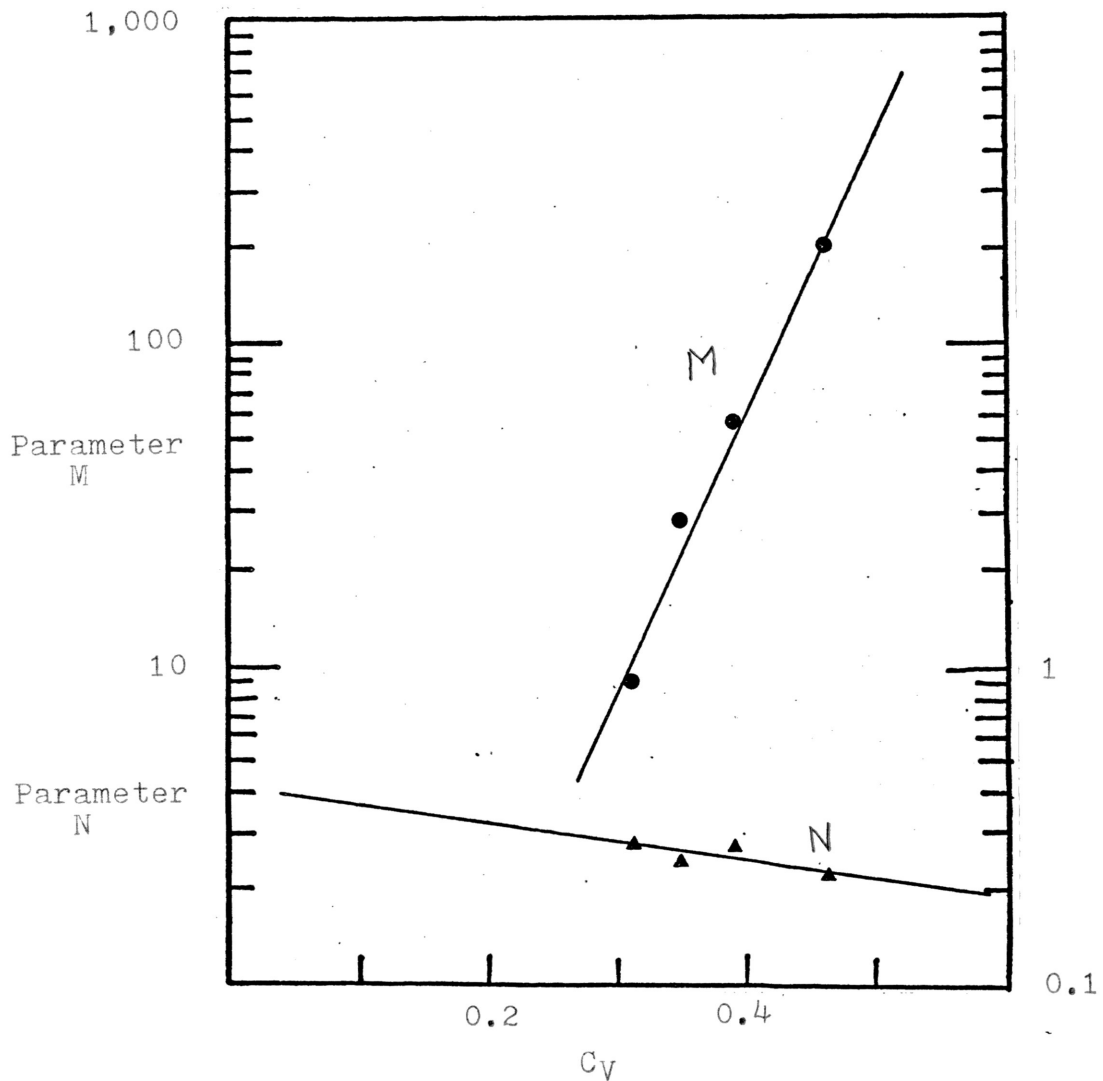


Fig. 23. Effect of Volume Fraction of Solids on Power Law Model For  $10^{-4}$  Molar NaCl

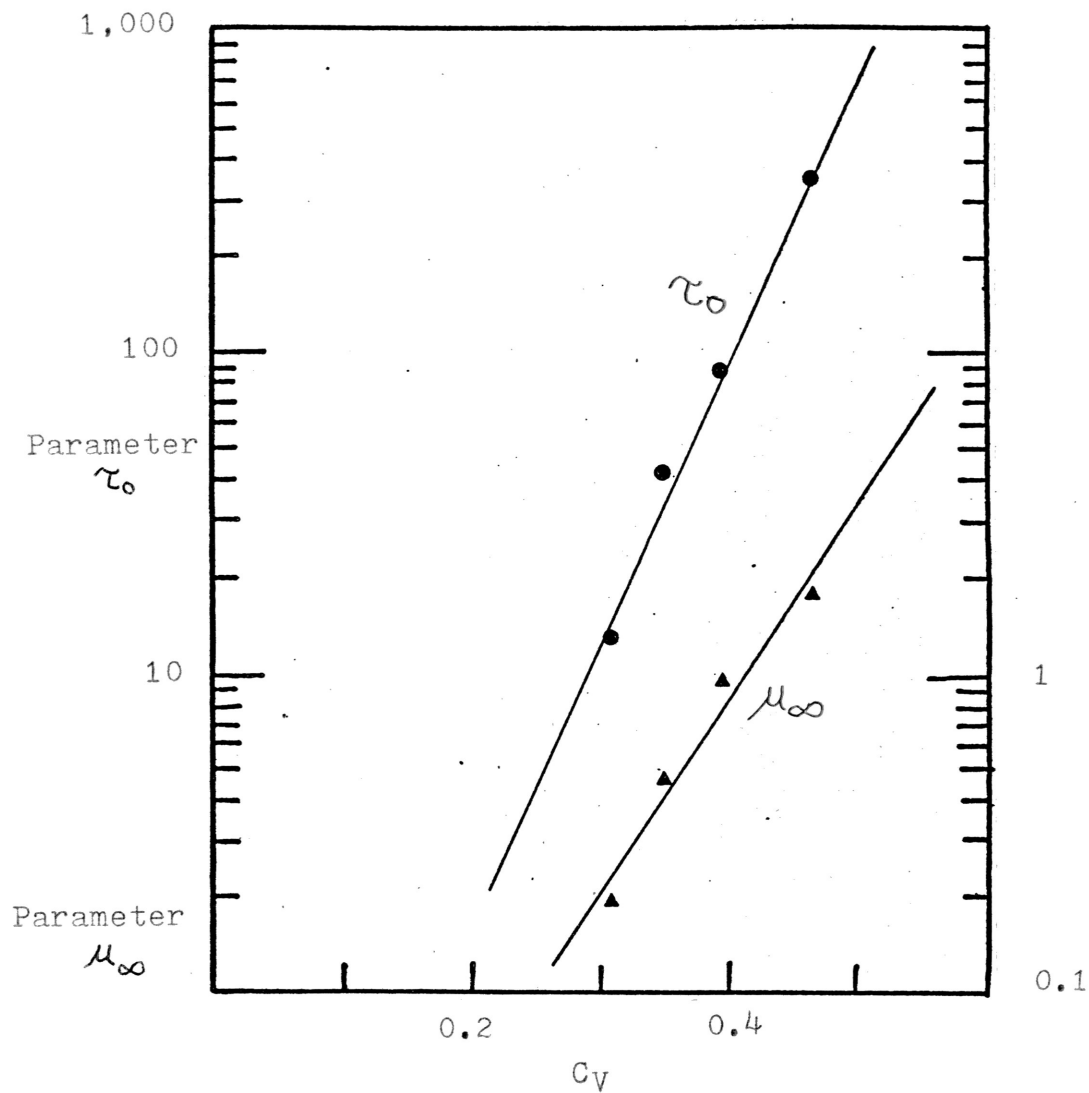


Fig. 24. Effect of Volume Fraction of Solids on Bingham Plastic Model For  $10^{-4}$  Molar NaCl

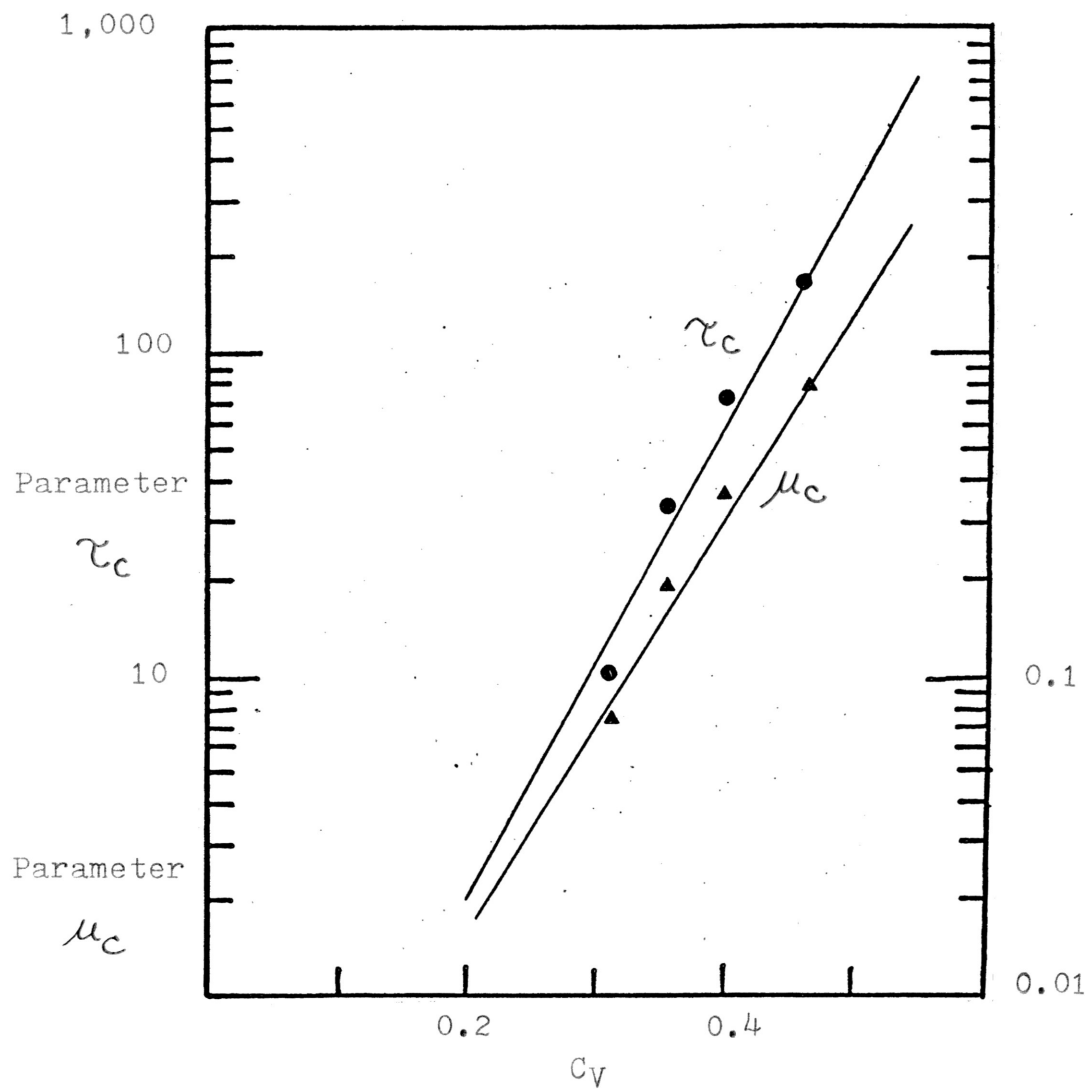


Fig. 25. Effect of Volume Fraction of Solids on Casson Model For  $10^{-4}$  Molar NaCl



TABLE 2

Values of the Constants A and B for Each Model Parameter

| MODEL   | PARAMETER | CONSTANT       | CONCENTRATION    |                  |                  |                  |        |
|---------|-----------|----------------|------------------|------------------|------------------|------------------|--------|
|         |           |                | 10 <sup>-1</sup> | 10 <sup>-2</sup> | 10 <sup>-3</sup> | 10 <sup>-4</sup> | Distil |
| Power   | M         | A              | .5404            | .0642            | .0131            | .0238            | .2074  |
|         |           | B              | 12.57            | 17.16            | 22.12            | 19.62            | 15.67  |
|         |           | r <sup>2</sup> | 0.94             | 0.86             | 0.89             | 0.98             | 0.91   |
| Power   | N         | A              | .4531            | .1500            | .2191            | .4084            | .2413  |
|         |           | B              | -2.32            | 1.07             | .146             | -1.21            | -.424  |
|         |           | r <sup>2</sup> | 0.71             | 0.37             | 0.03             | 0.63             | 0.16   |
| Bingham | $\tau_0$  | A              | .9275            | .0735            | .0138            | .0317            | .2843  |
|         |           | B              | 11.93            | 17.90            | 23.09            | 20.15            | 15.94  |
|         |           | r <sup>2</sup> | 0.92             | 0.88             | 0.89             | 0.99             | 0.92   |
| Bingham | $\mu_0$   | A              | .0214            | .0007            | .0006            | .0026            | .0043  |
|         |           | B              | 8.44             | 17.38            | 19.02            | 14.46            | 13.55  |
|         |           | r <sup>2</sup> | 0.77             | 0.96             | 0.93             | 0.94             | 0.92   |
| Casson  | $\tau_c$  | A              | 1.18             | .1079            | .0599            | .0528            | .4463  |
|         |           | B              | 10.65            | 16.06            | 17.98            | 17.61            | 13.55  |
|         |           | r <sup>2</sup> | 0.95             | 0.88             | 0.92             | 0.96             | 0.87   |
| Casson  | $\mu_c$   | A              | .0010            | 22.76            | .0002            | .0008            | .0011  |
|         |           | B              | 14.04            | -12.2            | 18.59            | 15.02            | 14.31  |
|         |           | r <sup>2</sup> | 0.88             | 0.37             | 0.94             | 0.96             | 0.64   |

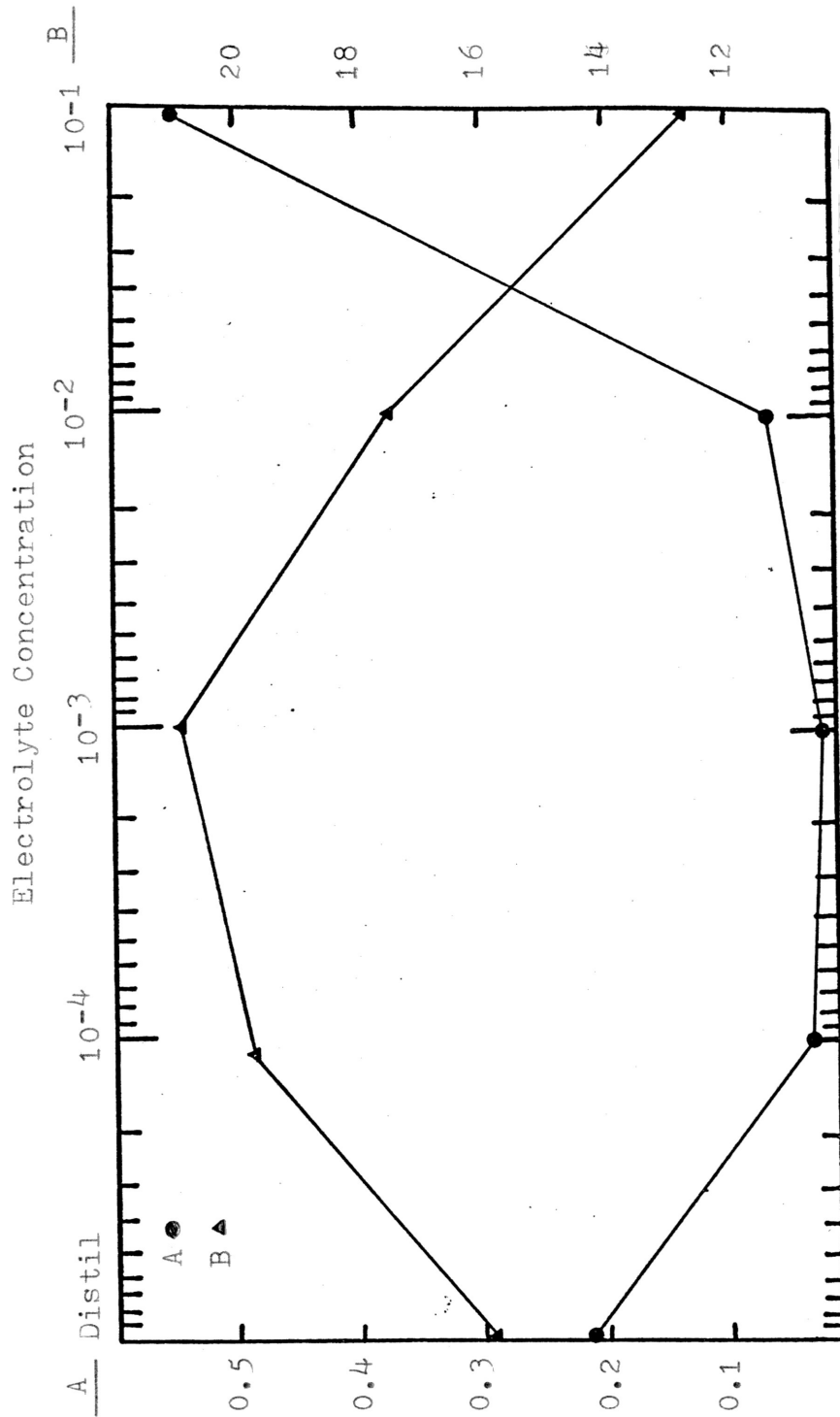


Fig. 26. The Effect of Electrolyte Concentration on the Parameter M From the Power Law Model

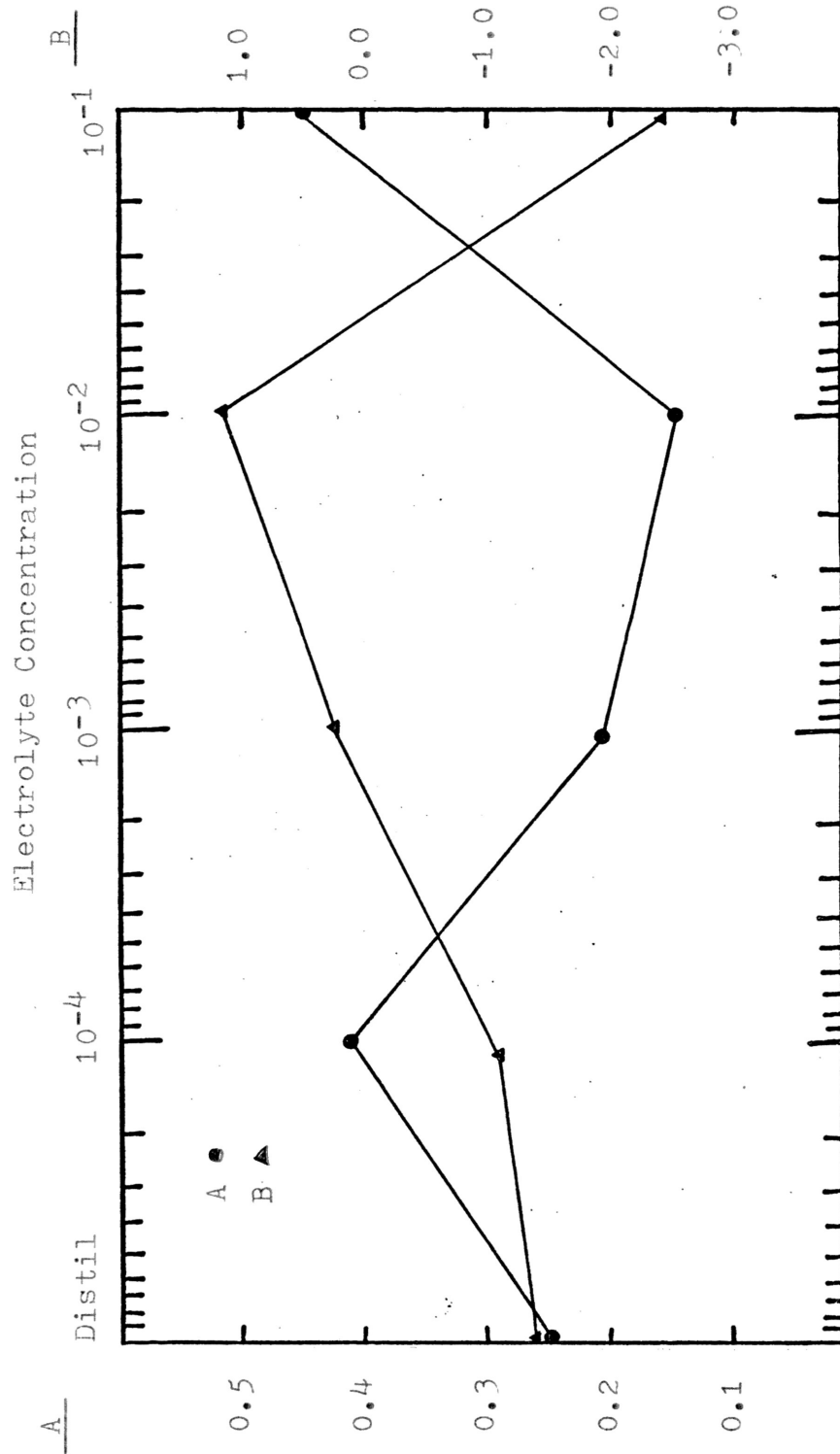


Fig. 27. The Effect of Electrolyte Concentration on the Parameter N From the Power Law Model

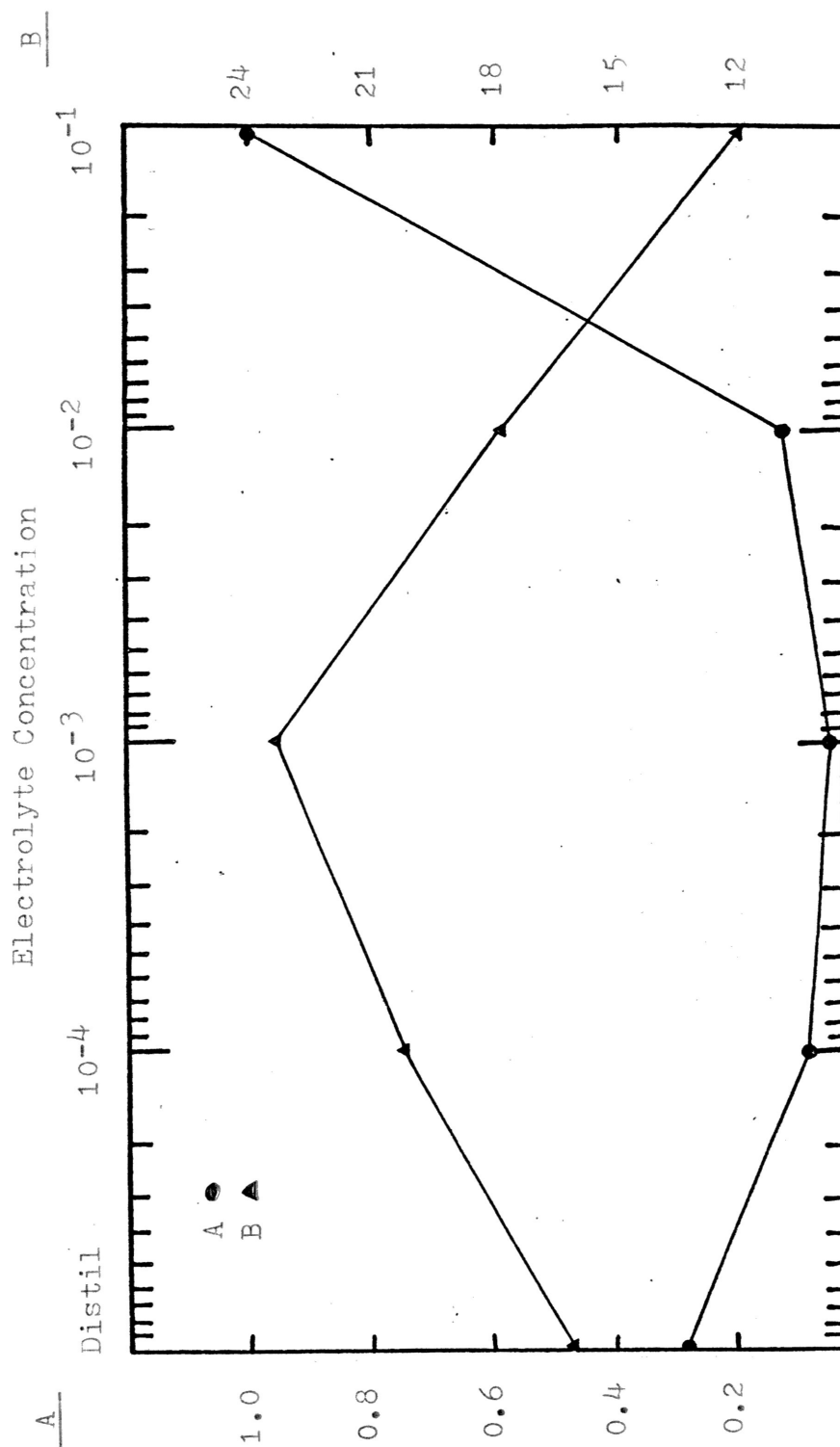


Fig. 28. The Effect of Electrolyte Concentration on the Parameter  $\tau_0$  From the Bingham Plastic Model

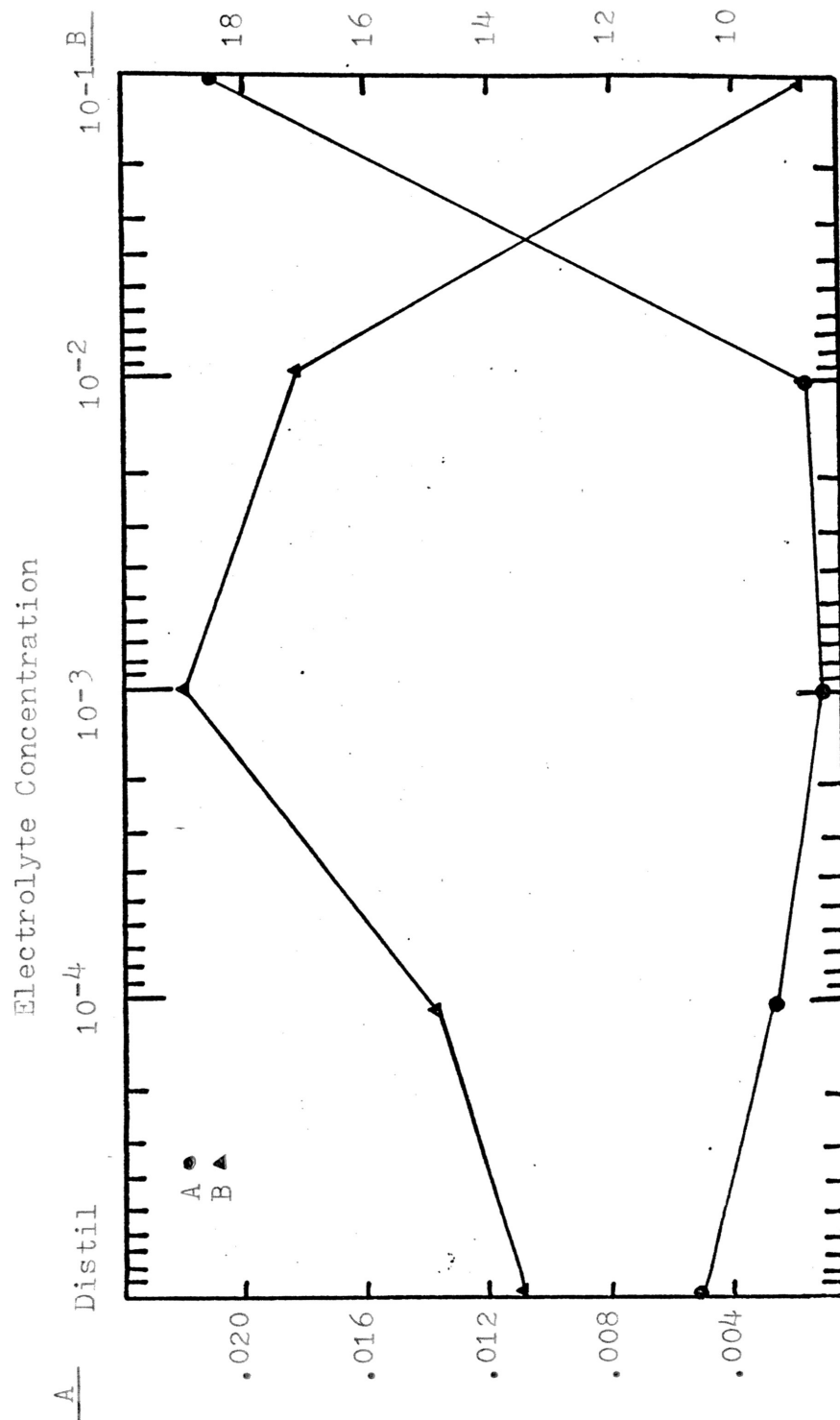


Fig. 29. The Effect of Electrolyte Concentration on the Parameter  $\mu_{\infty}$  From the Bingham Plastic Model

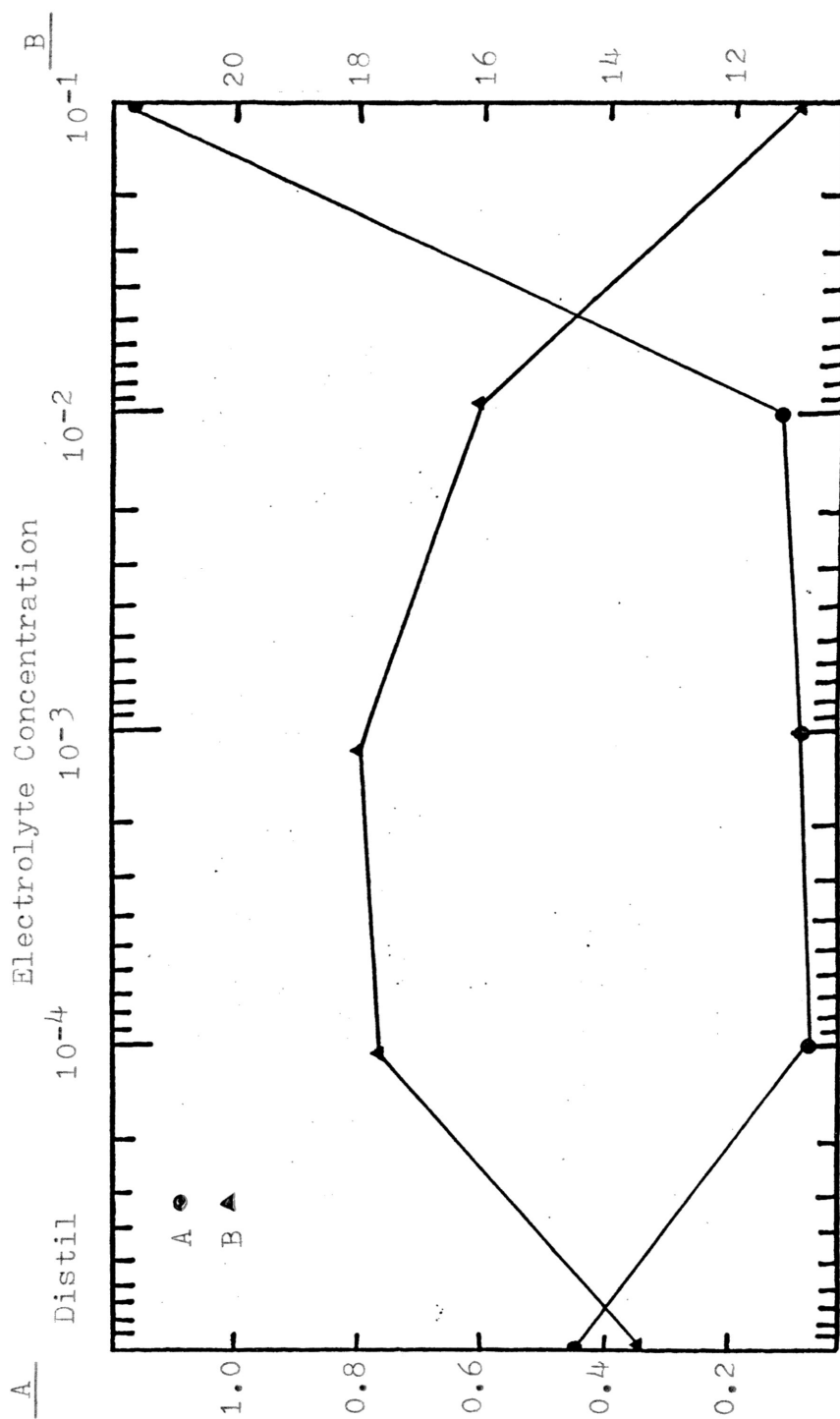


Fig. 30. The Effect of Electrolyte Concentration on the Parameter  $\tau_c$  From the Casson Model

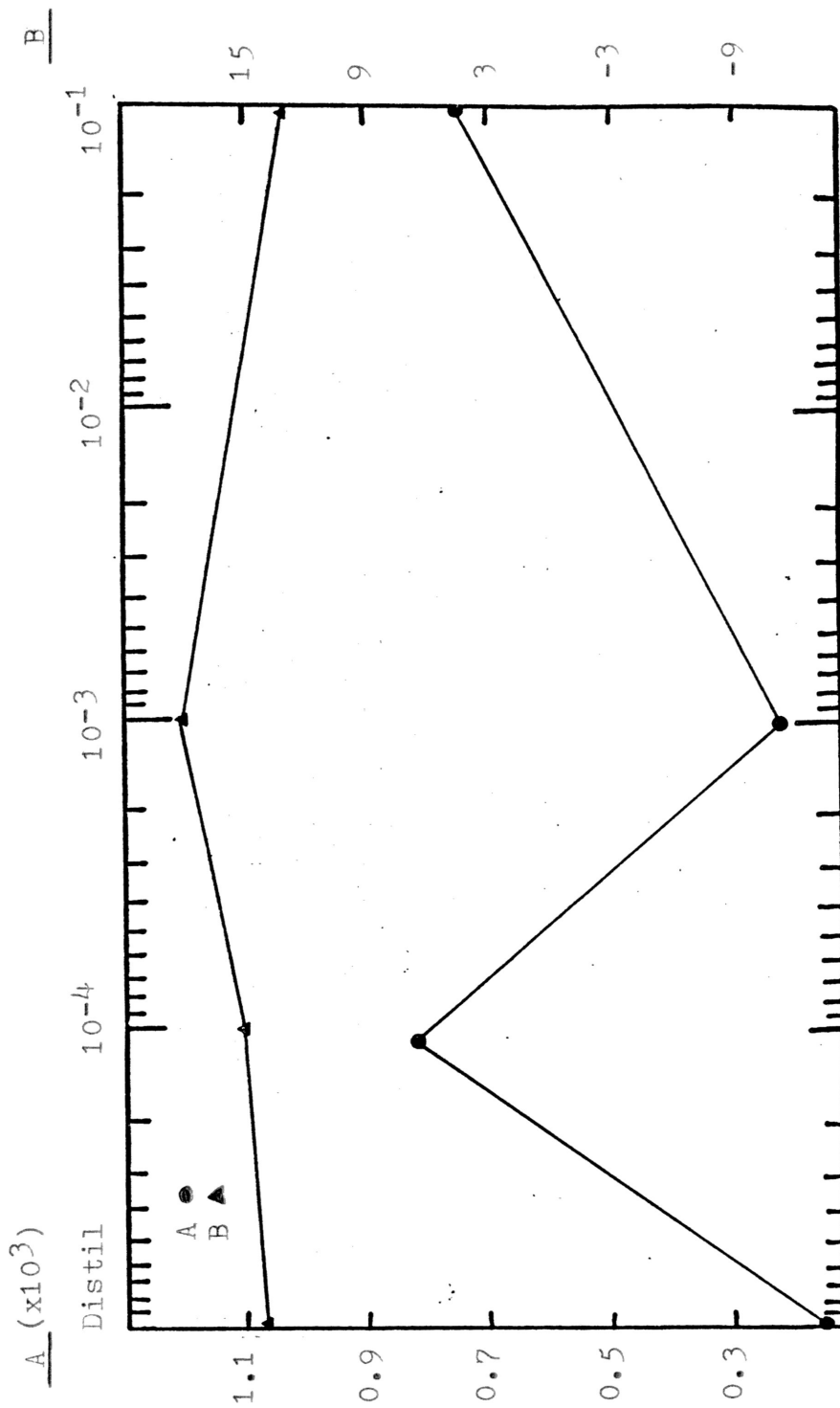


Fig. 31. The Effect of Electrolyte Concentration on the Parameter  $\mu_c$  From the Casson Model

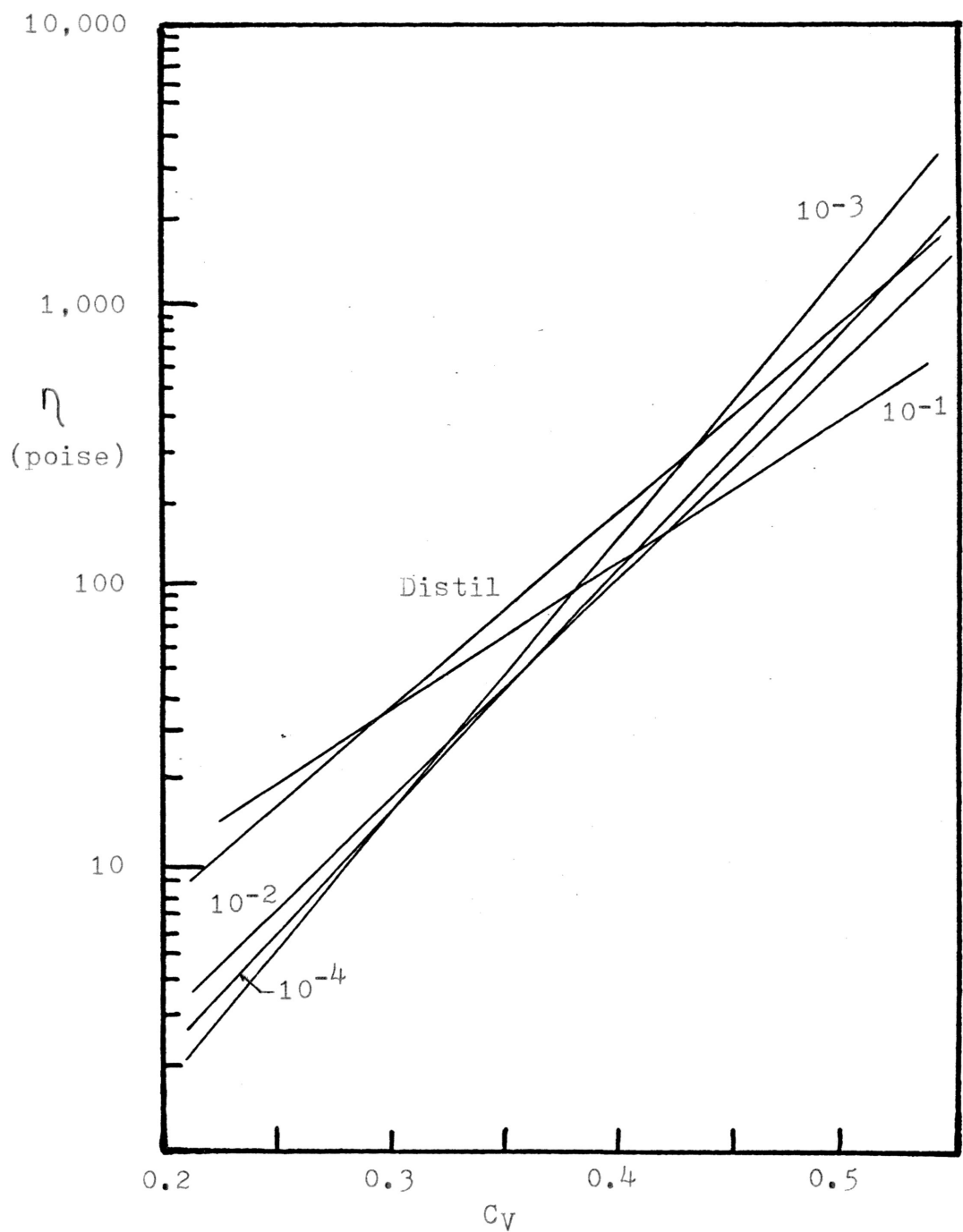


Fig. 32. The Effect of Volume Fraction of Solids and Electrolyte Concentration on Viscosity at a Constant Shear Rate of  $1 \text{ sec}^{-1}$



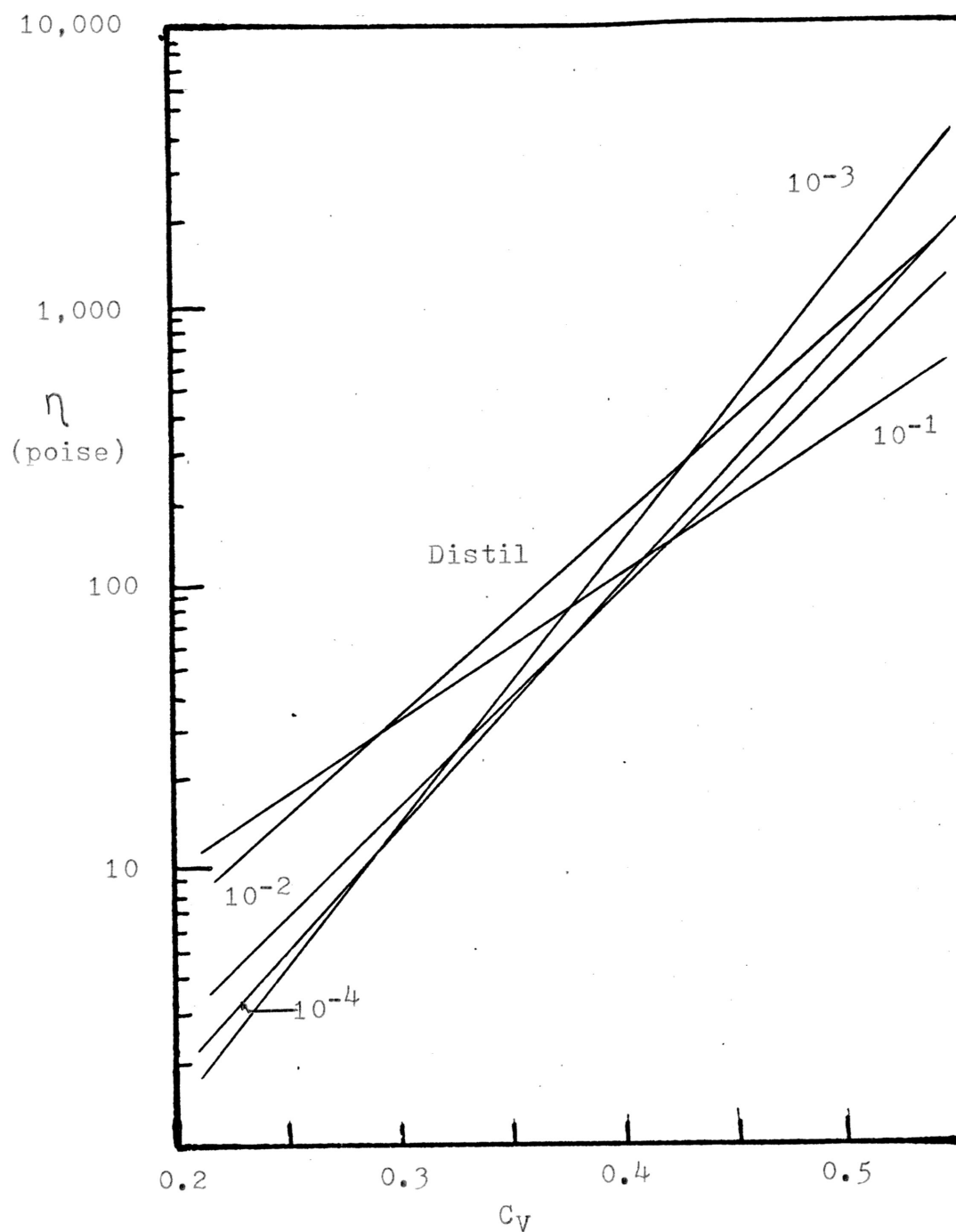


Fig. 33. The Effect of Volume Fraction of Solids and Electrolyte Concentration on Viscosity at a Constant Shear Rate of  $10 \text{ sec}^{-1}$

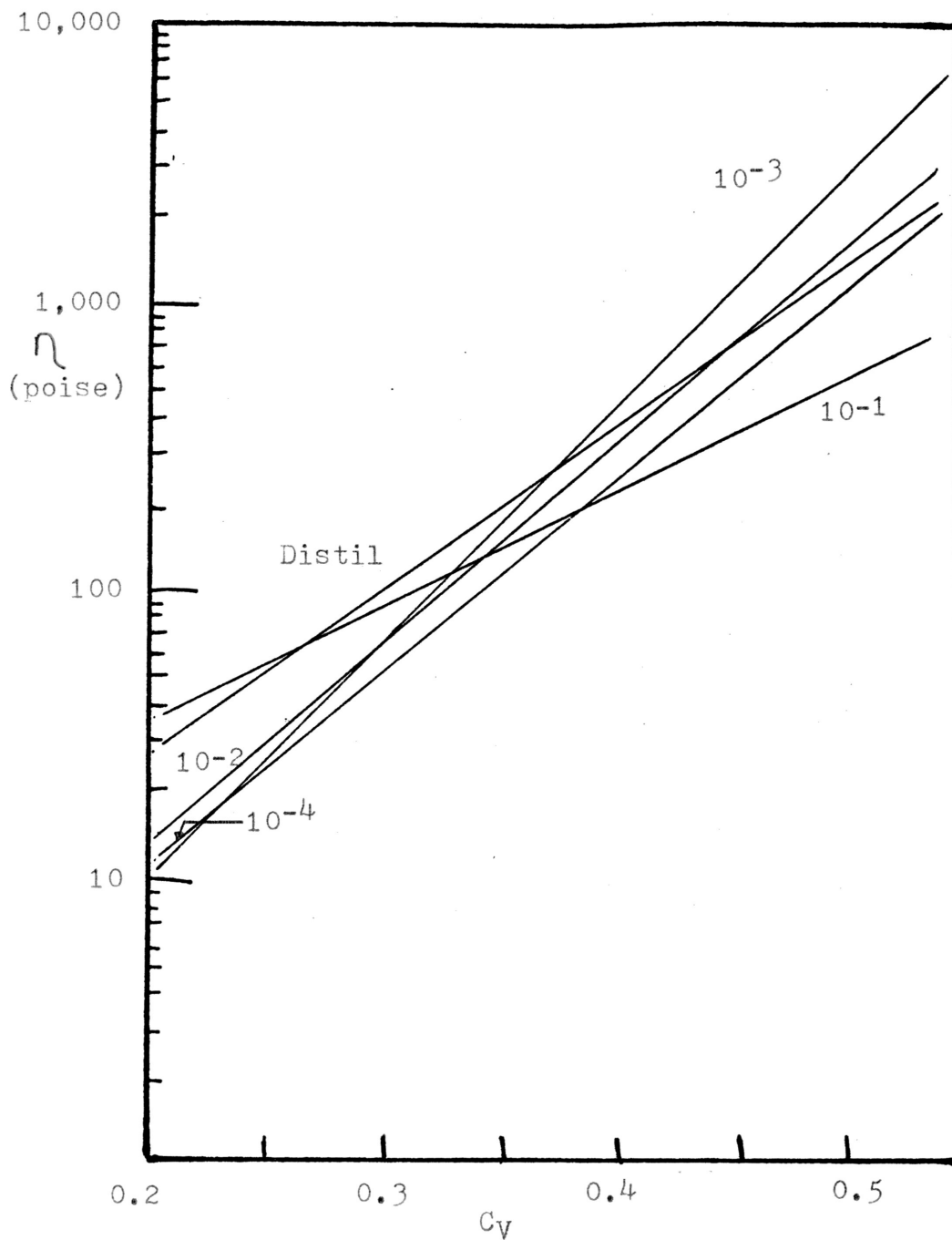


Fig. 34. The Effect of Volume Fraction of Solids and Electrolyte Concentration on Viscosity at a Constant Shear Rate of  $100 \text{ sec}^{-1}$

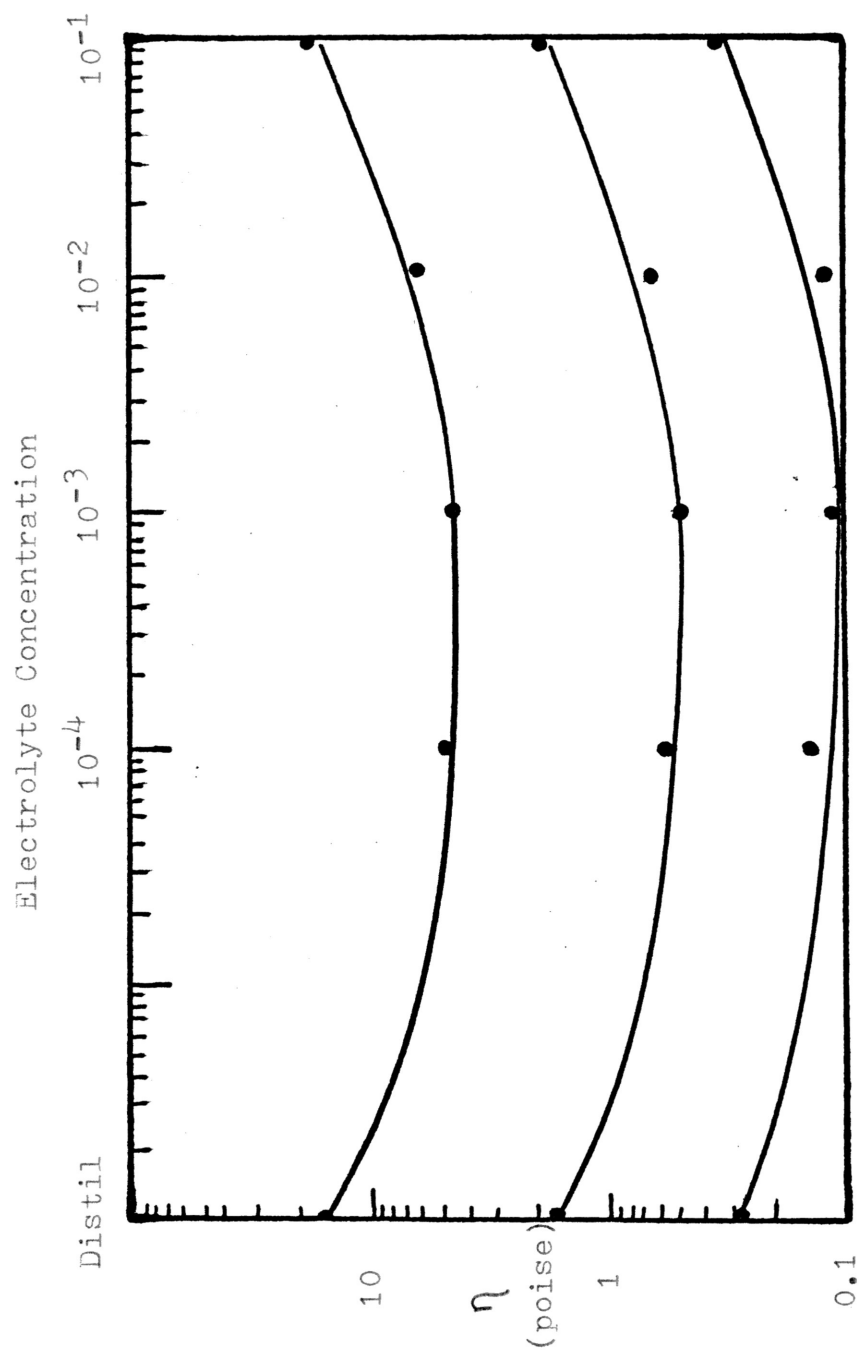


Fig. 35. The Effect of Electrolyte Concentration and Shear Rate on the Viscosity at a Constant Volume Fraction of Solids of 0.25

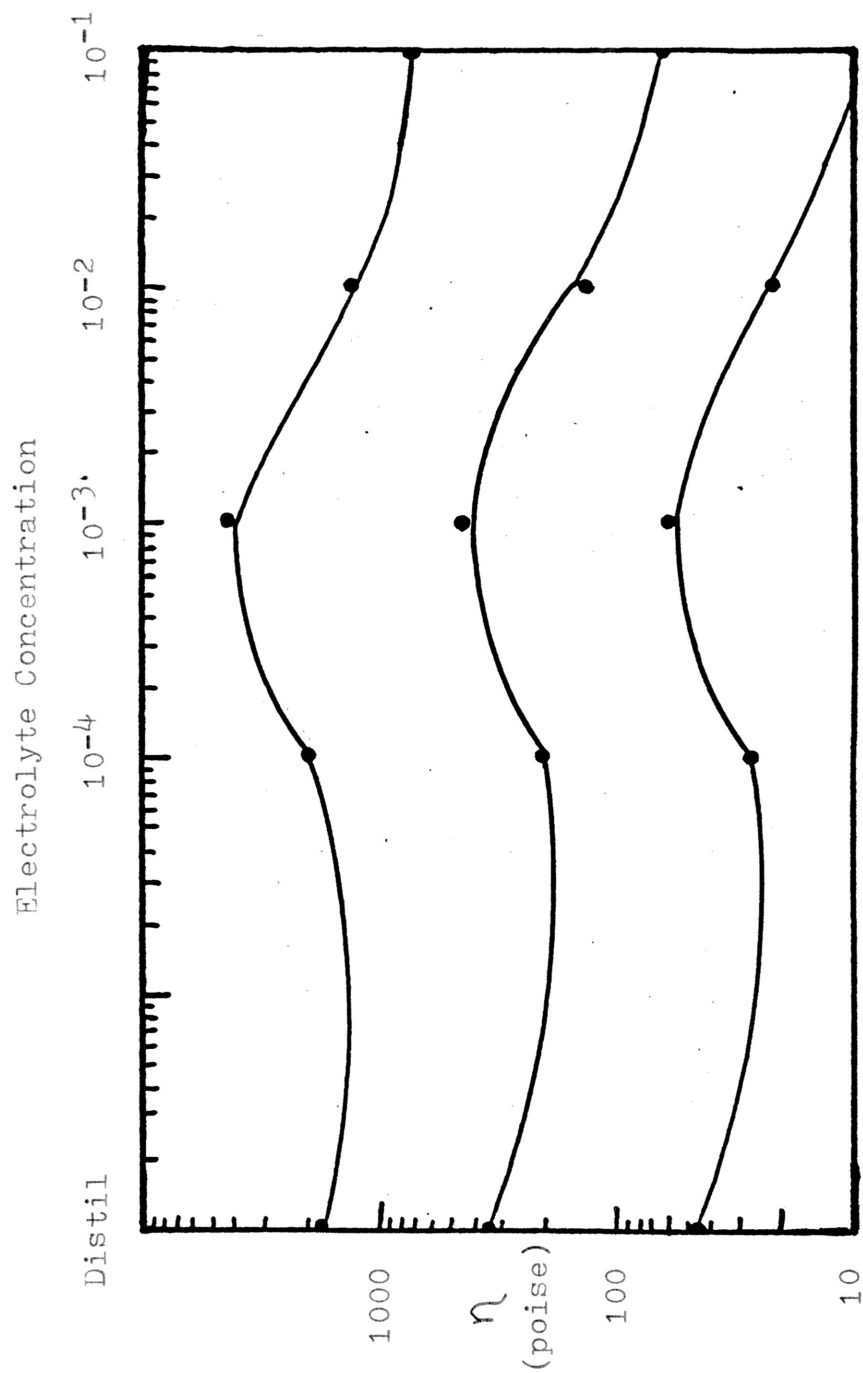


Fig. 36. The Effect of Electrolyte Concentration and Shear Rate on the Viscosity at a Constant Volume Fraction of Solids of 0.55

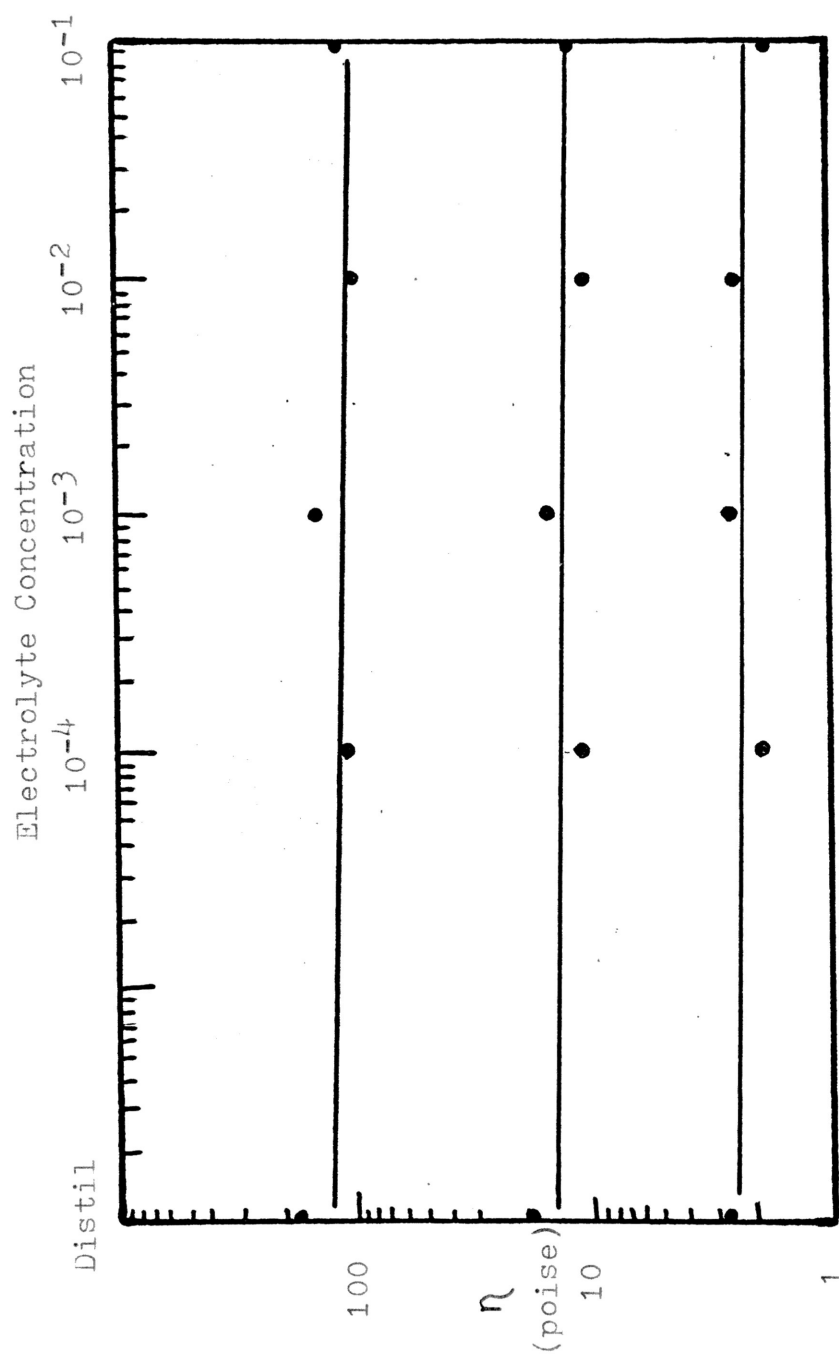


Fig. 37. The Effect of Electrolyte Concentration and Shear Rate on the Viscosity at a Constant Volume Fraction of Solids of 0.40

## CONCLUSIONS

1. Electrolyte concentration both decreased and increased suspension viscosity depending on the solids volume fraction of the suspension. At a low solids volume fraction of 0.25, the viscosity went through a minimum at an electrolyte concentration of  $10^{-3}$  molar then increased with further electrolyte addition. At a high solids volume fraction of 0.55, the suspension viscosity went through a maximum at  $10^{-3}$  molar electrolyte concentration and decreased with further electrolyte addition. Intermediate solids volume fractions showed no dependence to the electrolyte concentration.
2. The negatively charged  $\text{Cl}^-$  ion was adsorbed on the coal particle surface indicating that it is the negatively charged ions that interact with the particle double layer producing changes in the suspension viscosity.
3. The conductivity of the coal particles was so great that the electrolyte concentration had little effect on the overall suspension conductivity.
4. In analyzing electrolyte concentration effects on suspension viscosity, the Bingham Plastic Model best represented the experimental data.

## SUGGESTIONS FOR FURTHER STUDY

Through the course of the year, several other possibilities for further study were encountered. These fall into two main categories: variation of the electrolyte, and variation of the coal.

Studies of variation of the electrolyte type are needed to determine if particle interaction is independent of ion type or valence for coal suspensions. Subsequent studies should be extended to include such bivalent salts as magnesium chloride( $MgCl_2$ ), magnesium sulfate( $MgSO_4$ ), and sodium sulfate( $Na_2SO_4$ ). The fact that the coal particles were shown to adsorb the negative ion  $Cl^-$  would indicate that further studies should be concerned only with variations in the type and concentration of the negative ion added. Another study of interest would be the effect of an acid such as hydrochloric acid( $HCl$ ) on the apparent viscosity of coal suspensions. A better control sample could possibly be obtained by using deionized water instead of distilled water to ensure that no ions are initially present.

Variation in the type of coal studied is another area of continued interest. Coal from the Big Brown Mine is known to contain large amounts of clay. Clay minerals are also known to be negatively charged in their natural state. This inherent charge may have contributed to the

vigorous migration of the particles from the negative electrode. A harder coal with correspondingly less clay content may not exhibit such behavior. Since fewer negative charges are present, a higher electrolyte concentration may be necessary to achieve the same buffering effect on the particle double layer. Coals with varying hardness produce a range of particle size distributions different from that obtained in this work. Since the ionic double layer is affected by particle size, variation in the particle size distribution may produce changes in the effect of electrolytes on the apparent viscosity. A study of the actual adsorption process of the ions on the coal surface may help to quantitatively predict the viscosity response to various types and concentrations of ions.



## Literature Cited

1. Keller, L.J., U.S. Patent 4, 045, 092, August 30, 1977.
2. Fryling, Charles F., "The Viscosity of Small Particle, Electrolyte- and Soap-Deficient Synthetic Latex Gels", Journal of Colloid Science 18, 713-732 (1963)
3. Brodnyan, J.G., and Kelley, E.L., Journal of Colloid Science 20, 7 (1965)
4. Krieger, Irvin M., "The Second Electroviscous Effect in Polymer Latices", Transactions of the Society of Rheology, 20-1, 29-45 (1976)
5. Darby, R., Viscous Rheological Properties of Methacoal Suspensions from Texas Lignite, Final report to U.S. Department of Energy, pg 52, September, 1978.
6. Darby, R., Viscous Rheological Properties of Methacoal Suspensions from Texas Lignite, Final report to U.S. Department of Energy, pg 66, September, 1978.